

# Rare Semileptonic Charmed $B$ meson decay in the Standard Model and Beyond

by

**Ibad Ur Rehman**



A thesis submitted for the degree of Master of Science  
in Physics

Supervised by

**Dr. Muhammad Ali Paracha**

**School of Natural Sciences (SNS)**

National University of Sciences and Technology,  
H-12, Islamabad, Pakistan


© Ibad Ur Rehman, 2020

**National University of Sciences & Technology****MS THESIS WORK**

We hereby recommend that the dissertation prepared under our supervision by: Mr. Ibad Ur Rehman, Regn No. 00000278278 Titled: "Rare Semileptonic Charmed B Meson Decays in the Standard Model and Beyond" be accepted in partial fulfillment of the requirements for the award of MS degree.

**Examination Committee Members**1. Name: Dr. Rizwan KhalidSignature: 2. Name: Dr. Fahad AzadSignature: External Examiner: Dr. Shabbar RazaSignature: Supervisor's Name: Dr. Muhammad Ali ParachaSignature: 

Head of Department

  
Date**COUNTERSIGNED**Date: 20/10/2020  
Dean/Principal

## THESIS ACCEPTANCE CERTIFICATE

Certified that final copy of MS thesis written by **Mr. Ibad Ur Rehman**, (Registration No. **00000278278**), of **School of Natural Sciences** has been vetted by undersigned, found complete in all respects as per NUST statutes/regulations, is free of plagiarism, errors, and mistakes and is accepted as partial fulfillment for award of MS/M.Phil degree. It is further certified that necessary amendments as pointed out by GEC members and external examiner of the scholar have also been incorporated in the said thesis.

Signature: \_\_\_\_\_ 

Name of Supervisor: Dr. Muhammad Ali Paracha

Date: 20/10/2020

Signature (HoD): \_\_\_\_\_ 

Date: 20/10/2020

Signature (Dean/Principal): \_\_\_\_\_ 

Date: 20/10/2020

---

Dedicated to my loving parents

# Acknowledgment

I express my profound gratitude to my supervisor **Dr. Muhammad Ali Paracha** for his dynamic supervision and valuable support throughout course work and research. He always responded to my questions and queries so promptly and efficiently. I would like to thank my Guidance and Examination Committee (GEC) members, **Dr. Rizwan Khalid** and **Dr. Fahad Azad**, for their kind support, encouragement and insightful comments. I would like to thank, **Dr. Saadi Ishaq**, for their encouragement and numerous valuable discussions that he made with me.

I was very fortunate to be a student in the nurturing environment of School of Natural Sciences (SNS). I am thankful to all of my teachers at SNS, especially, Head of department of Physics, **Dr. Shahid Iqbal**, for their kind support and valuable guidance throughout my degree.

I am grateful to my mentor, **Prof. Asghar Qadir**, for his sympathetic attitude and I learnt a lot of things from him during my course work.

I am also thankful to my friends and fellows. I am grateful to my parents and siblings those have been a constant source of support and encouragement.

Ibad Ur Rehman.

# Abstract

Motivated by anomalies in lepton flavor universality ratios for  $B \rightarrow D^{(*)}\tau\nu$  and  $B \rightarrow K^{(*)}\mu^+\mu^-$  decays which have found deviations,  $2.1-2.3\sigma$  and  $2.6\sigma$ , from standard model(SM) predictions, the deviations between experimental measurements and SM prediction which hint towards new physics(NP) effects.

In this thesis, we study exclusive semileptonic charmed  $B$  meson decay,  $B_c \rightarrow D_s^*\ell^+\ell^-$ , with in the SM and beyond which provides a complimentary information regarding NP. We consider the simplest NP models such as,  $Z'$  models and model independent/Leptoquark model. We analyze various observables such as the branching ratios, leptons forward backward asymmetry, the longitudinal helicity fractions of the  $D_s^*$  meson and lepton flavor Universality(LFU) ratios with in the SM and the above mentioned NP models. We give a combine analysis of model independent NP scenarios and  $Z'$  models for above mentioned observables which also deviate from the SM predictions and hints the NP effects in  $B_c \rightarrow D_s^*\ell^+\ell^-$  decay.

# Contents

|   |           |
|---|-----------|
| <b>Contents</b>   | <b>1</b>  |
| <b>List of Tables</b>   | <b>3</b>  |
| <b>List of Figures</b>  | <b>4</b>  |
| <b>1 Introduction</b>   | <b>5</b>  |
| <b>2 Standard Model</b>   | <b>7</b>  |
| 2.1 Gauge Theory . . . . .  | 7         |
| 2.2 The Standard Model Lagrangian . . . . .   | 8         |
| 2.2.1 Gauge Symmetry Group . . . . .  | 8         |
| 2.2.2 Fermionic Field in SM . . . . .   | 9         |
| 2.2.3 Higgs Lagrangian . . . . .  | 11        |
| 2.2.4 Higgs Mechanism . . . . .   | 11        |
| 2.2.5 Higgs and Yukawa Terms . . . . .  | 12        |
| 2.3 CKM matrix and Fermion masses . . . . .   | 13        |
| <b>3 Theoretical Framework for <math>B</math> Meson Decay</b>                         | <b>17</b> |
| 3.1 Effective Field Theory . . . . .  | 17        |
| 3.1.1 Operator Product Expansion . . . . .  | 18        |
| 3.2 Effective Hamiltonian . . . . .   | 19        |
| 3.3 Model Independent Scenarios . . . . .   | 21        |
| 3.3.1 Leptoquark Model . . . . .  | 22        |
| 3.3.2 $Z'$ Model . . . . .  | 23        |
| 3.3.3 Heavy $Z'$ Model . . . . .  | 24        |
| 3.3.4 Light $Z'$ Model . . . . .  | 25        |
| <b>4 Analysis of Decay <math>B_c \rightarrow D_s^* \ell^+ \ell^-</math> Beyond SM</b> | <b>26</b> |
| 4.1 Effective Hamiltonian of decay $B_c \rightarrow D_s^* \ell^+ \ell^-$ . . . . .    | 26        |
| 4.2 Matrix Element and Form Factors . . . . .   | 28        |
| 4.3 Helicity Amplitude of B meson decay . . . . .                                     | 28        |
| 4.3.1 Hadronic part . . . . .   | 31        |

|          |  |           |
|----------|--|-----------|
| 4.3.2    | Leptonic Part . . . . .  | 32        |
| 4.4      | Differential decay rate . . . . .  | 33        |
| 4.5      | Forward Backward Asymmetry . . . . .   | 34        |
| 4.6      | Helicity Fraction . . . . .  | 35        |
| 4.7      | Lepton Flavor Universality Ratios . . . . .  | 35        |
| 4.8      | Phenomenological Analysis . . . . .  | 36        |
| 4.8.1    | Predictions for $R_{D_s^*}$ , $R_{D_s^*}^{L,T}$ , $F_{D_s^*}^L$ , $A_{FB}$ in Different $q^2$ Bins . . . . . | 38        |
| <b>5</b> | <b>Conclusion</b>  | <b>44</b> |
|          | <b>Bibliography</b>  | <b>45</b> |



# List of Tables

|     |   |    |
|-----|---|----|
| 2.1 | The Standard Model Bosons . . . . .   | 9  |
| 2.2 | Standard Model fermions . . . . .   | 10 |
| 3.1 | MI scenarios: WCs values in best fitting are taken from ref. [1] . . . . .  | 22 |
| 3.2 | TeV Heavy $Z'$ model in best fit values of $a_L^{bs}$ in fit A in Ref. [1] . . . . .  | 24 |
| 3.3 | TeV Heavy $Z'$ model in best fit values of $a_L^{bs}$ in fit B in Ref. [1] . . . . .  | 25 |
| 3.4 | GeV Light $Z'$ model in best fit values of $a_L^{bs}$ in fit A in Ref. [1] . . . . .  | 25 |
| 4.1 | Form factors of $B_c \rightarrow D_s^*$ decay which are calculated by using QCD Sum rules [2]. . . . .  | 29 |
| 4.2 | In different $q^2$ bins: averaged values in different observables of $B_c \rightarrow D_s^* \mu^+ \mu^-$ decay in the SM. . . . .                   | 36 |
| 4.3 | The values of WCs $\mathcal{C}_i(\mu)$ [2] at the scale $\mu = 4.8 GeV$ shown in above table. . . . .   | 36 |
| 4.4 | Predictions in SM and NP: Lepton flavor universality ratios $R_{D_s^*}$ in different bin values for $B_c \rightarrow D_s^* \mu^+ \mu^-$ . . . . .   | 41 |
| 4.5 | Predictions in SM and NP: Lepton flavor universality ratios $R_{D_s^*}^L$ in different bin values for $B_c \rightarrow D_s^* \mu^+ \mu^-$ . . . . . | 42 |
| 4.6 | Predictions in SM and NP: Lepton flavor universality ratios $R_{D_s^*}^T$ in different bin values for $B_c \rightarrow D_s^* \mu^+ \mu^-$ . . . . . | 42 |
| 4.7 | Predictions in SM and NP: Longitudinal helicity fraction $F_{D_s^*}^L$ in different bin values for $B_c \rightarrow D_s^* \mu^+ \mu^-$ . . . . .    | 43 |
| 4.8 | Predictions in SM and NP: Forward backward asymmetry $A_{FB}$ in different bins for $B_c \rightarrow D_s^* \mu^+ \mu^-$ . . . . .                   | 43 |

# List of Figures

|     |   |    |
|-----|---|----|
| 3.1 | Left shows full theory and at Right the effective theory in $c \rightarrow s u \bar{d}$ . . . . .   | 18 |
| 3.2 | Effective diagram of $b \rightarrow s \ell^+ \ell^-$ . . . . .  | 19 |
| 4.1 | Penguin diagram for $B_c \rightarrow D_s^* \ell^+ \ell^-$ decay [3] . . . . .   | 26 |
| 4.2 | Branching ratio in MI Scenarios, Leptoquark Model, Heavy $Z'$ Model and Light $Z'$ Model. The Gray band show the predictions in the SM, Blue, Brown, Yellow and Magenta(dashed) bands show the predictions computed in MI scenario I(A), I(B), II(A) and II(B) respectively. Green, Red(dashed), Blue(dashed) and Cyan bands show the predictions computed in scenario $HZ'$ I(A), $HZ'$ I(B), $HZ'$ II(A) and $HZ'$ II(B) respectively. Purple and Orange bands shows the predictions in scenario $LZ'$ I(A), $LZ'$ II(A) respectively. The results achieved in MI scenarios II(A) and II(B) also represent the results in leptoquark model. . . . . | 39 |
| 4.3 | Leptons forward backward asymmetry in MI Scenarios, LQ Model, Heavy $Z'$ Model and Light $Z'$ Model. The legends are same as in fig.4.2 . . . . .   | 40 |
| 4.4 | Longitudinal helicity fraction of $D_s^*$ in MI Scenarios, LQ Model, Heavy $Z'$ Model and Light $Z'$ Model. The legends are same as in fig.4.2 . . . . .  | 41 |

# Introduction

The standard model (SM) [4] was proposed by Salam, Glashow and Weinberg to unify weak nuclear forces and electromagnetism. Many years have passed since the SM was established. It is a miracle that it still holds the status as the ultimate theory of matter at the most fundamental level. The SM provides a very elegant theoretical framework and it is experimentally well tested theory so far. Despite the successful theory of SM, it has some limitations and some unanswered questions:

- The SM shows the neutrinos are massless, in fact experiment shows that neutrinos have mass.
- Hierarchy problem: Electroweak scale is so small?
- The problem of strong CP violation.
- There is lack of explanation for the quark masses according to their ranges i.e. few MeV to 100 GeV and lepton masses i.e. 0.5 MeV to 1.8 GeV.
- Why gravity is missing from SM?

These limitations and unanswered questions required more fundamental underlying theory. Many extension of SM discussed in literature to understand these limitations and unanswered questions of SM. These problems also hint that new physics (NP) effects may become important beyond the SM. Generally, there are two methods to find NP: First, we can rise the energy of colliders and produce new particles, this is called a direct method. Second, there is the indirect way to determine NP where NP effects can appear itself if we increase the experimental precision on data of SM processes. These processes can be measured precisely because it is rare in SM. So here flavor physics plays its important role. In such a way the flavor changing processes are important to understand the physics beyond the SM. It implies that such processes in the flavor sector are rare  $B$  meson decays which are mediated by flavor changing neutral current (FCNC) [5] at loop level based on the Glashow-Iliopoulos-Maiani

(GIM) mechanism [6]. So, rare  $B$  meson [7] decays are ideal tool to test NP due to their intrinsic relation to the quark flavor structure of the SM Lagrangian.

$B$  meson are bound state of  $(b\bar{q})$ . In our dissertation, we focus on rare  $B_c$  meson, the initial state  $B_c$  meson is the ground state of the bottom-charm bound system. Its first observation was at the Fermilab Tevatron by the CDF Collaboration in 1998 through the cascade decay  $B_c \rightarrow J/\psi \bar{l} \nu$  and  $J/\psi \rightarrow \mu \bar{\mu}$  [3].

In this thesis, we analyze exclusive semileptonic  $B$  meson decay  $B_c \rightarrow D_s^* \bar{l} l$  [3] based on quark level transition  $b \rightarrow s \ell^+ \ell^-$  induced by FCNC at loop level. In the Standard Model, these transitions occur at loop level mediated by  $W$  boson and are not allowed at tree level. Furthermore, they are also suppressed in the SM due to their dependence on weak mixing angles of the Cabibo Kobayashi Maskawa (CKM) matrix [8]. It implies that the SM contribution is greatly suppressed and, as the SM contribution is suppressed, the NP effects may become important. This provides the most crucial framework to test the SM. As the quark level  $b \rightarrow s \ell^+ \ell^-$  transition are very sensitive to the physics beyond the SM, so it offers a promising place to search for NP.

We consider only those NP models where the effects of NP can be observed only through the modification of Wilson coefficients. we consider two different NP models such as leptoquark model, heavy and light  $Z'$  models, and Model independent(MI) NP scenarios.

Several observables are useful to distinguish between the various extension of SM. We determined various observables such as branching ratio, forward backward asymmetry of leptons, longitudinal helicity fraction of  $D_s^*$  meson and lepton flavor universality ratios of leptons which show the deviations form SM predictions.

The purpose of this dissertation is to study the possibility of finding NP in MI scenarios and in Leptoquark and  $Z'$  models. When more data will be available at LHC than the study of above mentioned observables will give a precision test of SM and NP .

We organized our dissertation as given below:

In Chapter 2, we give an overview of the SM. We put our focus on the fundamental particles, their parameters and interactions such as masses and coupling constants and we precisely deal with the flavor structure of SM which help us to understand rare  $B$  meson decays.

In Chapter 3, we present the theoretical framework for rare  $B$  meson decays. Firstly, we write the effective Hamiltonian which is the fundamental of this thesis than we explain how effective field theory is important to compute said process. We compute the amplitude of said decay in helicity basis by using effective Hamiltonian and will be able to write the decay rate of  $B_c \rightarrow D_s^* \ell^+ \ell^-$ . In next section, we explore physics beyond SM. We wil do combine analysis of NP models such as, leptoquark and  $Z'$  models, and model independent new physics scenarios.

In Chapter 4, we determine several observables for exclusive semileptonic  $B_c \rightarrow D_s^* \ell^+ \ell^-$  decay mode, like branching ratio, longitudinal helicity fraction of  $D_s^*$  meson, forward backward asymmetry and Lepton Flavor Universality(LFU) ratios which help us to understand new physics in said process. We analyze the above mentioned physical observables in NP model independent scenarios and in model dependent and will show that above mentioned observables have tension with SM predictions. In last chapter, we summarize all our results and discussions.

# Standard Model

The Standard Model(SM) [4] corresponds to a non-abelian gauge principle [9], it is a quantum field theory based upon local gauge invariance. The SM consists of strong and electroweak interactions which is based on the gauge symmetry  $SU(3)_C \otimes SU(2)_L \otimes U(1)_Y$ .  $SU(3)_C$  has the symmetry group of strong interactions and  $SU(2)_L \otimes U(1)_Y$  has the symmetry group of electroweak interactions. The SM provides a basic theoretical framework and it is experimentally well tested theory so far. Despite the successful theory of SM, it has some limitations and some unanswered questions which we will discuss later.

## 2.1 Gauge Theory

Gauge principle give a tool to transform Lagrangian that is invariant with respect to global symmetry transformation of non-abelian symmetric  $SU(N)$  group into a Lagrangian that consists of a local symmetry invariance. Suppose a Lagrangian  $\mathcal{L}(\Psi(y), \partial_\mu \Psi(y))$  which is invariant under  $SU(N)$  *global transformation*.

$$\Psi(y) \rightarrow U\Psi(y), \quad U^{-1} = U^\dagger. \quad (2.1)$$

But our desire to develop a theory i.e. invariant with respect to local  $SU(N)$  transformation

$$\Psi(y) \rightarrow U(y)\Psi(y), \quad U = e^{i\alpha^a(y)X^a} \quad (2.2)$$

The Lagrangian is now no more invariant under this local transformation. To preserve the local invariance, we introduce the covariant derivative  $\mathcal{D}_\mu$

$$\mathcal{D}_\mu = \partial_\mu - igA_\mu^a X^a \quad (2.3)$$

transform as

$$\mathcal{D}_\mu \Psi(y) \rightarrow (\mathcal{D}_\mu \Psi(y))' = U(y)(\mathcal{D}_\mu \Psi(y))$$

Where  $g$  is the arbitrary constant defined as coupling constant,  $A_\mu^a$  defined as a vector fields or it is also called gauge fields and  $X^a$  are the corresponding generators that follow the commutation algebra

$$[X^a, X^b] = if^{abc} X^c$$

$f^{abc}$  define as the structure constant. To restore gauge invariance,  $A_\mu$  vector field transforms as

$$A_\mu^a \rightarrow A_\mu^{a'} = U(y)(A_\mu^a + \frac{i}{g}\partial_\mu)U^\dagger(y).$$

Finally, by adding the *kinetic term* for gauge field: Introducing locally invariant term that depends on  $A_\mu$  and its derivative. The field strength tensor  $F^{\mu\nu}$  looks like

$$F^{\mu\nu,a} = \partial^\mu A^{\nu,a} - \partial^\nu A^{\mu,a} + gf^{abc} A^{\mu,b} A^{\nu,c}.$$

The product of  $F^{\mu\nu,a} F_{\nu\mu}^a$  satisfies the structure of gauge theory and appears into the Lagrangian.

The new locally invariant Lagrangian takes the following form

$$\mathcal{L} = \mathcal{L}(\Psi(y), \mathcal{D}_\mu \Psi(y)) - \frac{1}{4} F^{\mu\nu} F_{\nu\mu}. \quad (2.4)$$

The Gauge theory principle extended a global to local symmetry and it give an information about gauge field interactions.

## 2.2 The Standard Model Lagrangian

The SM Lagrangian [10] consists of the following main pieces

$$\mathcal{L} = \mathcal{L}_{gauge} + \mathcal{L}_{fermions} + \mathcal{L}_{higgs} + \mathcal{L}_{yukawa} \quad (2.5)$$

$\mathcal{L}_{gauge}$ ,  $\mathcal{L}_{fermions}$ ,  $\mathcal{L}_{higgs}$  and  $\mathcal{L}_{yukawa}$  terms correspond to the gauge group  $SU(3)_c \otimes SU(2)_L \otimes U(1)_Y$ , the matter contents of fermions, the Higgs sector and the coupling of Higgs with fermion of SM respectively.

### 2.2.1 Gauge Symmetry Group

The SM Lagrangian [11,12] is established on symmetry group  $SU(3)_c \otimes SU(2)_L \otimes U(1)_Y$ . The  $SU(3)_c$  color symmetry group explains the strong interaction between quarks corresponding to quantum chromodynamic (QCD) part. The  $SU(2)_L \otimes U(1)_Y$  gauge group explains the Glashow-Weinberg-Salam electroweak interaction theory. The gauge terms Lagrangian is as follows

$$\mathcal{L}_{gauge} = -\frac{1}{4} B_{\mu\nu} B^{\mu\nu} - \frac{1}{4} W_{\mu\nu}^i W^{i,\mu\nu} - \frac{1}{4} G_{\mu\nu}^a G^{a,\mu\nu} \quad (2.6)$$

The field strength tensor defined as

$$\begin{aligned} B_{\mu\nu} &= \partial_\mu B_\nu - \partial_\nu B_\mu \\ W_{\mu\nu}^i &= \partial_\mu W_\nu^i - \partial_\nu W_\mu^i + g_2 \epsilon^{ijk} W_\mu^j W_\nu^k \\ G_{\mu\nu}^a &= \partial_\mu G_\nu^a - \partial_\nu G_\mu^a + g_3 f^{abc} G_\mu^b G_\nu^c \end{aligned}$$

Where  $W_\mu^i (i = 1, 2, 3)$  and  $G_\mu^a (a = 1, \dots, 8)$ , and the corresponding covariant derivatives are

$$\begin{aligned} D_\mu &= \partial_\mu - ig_1(Y)B_\mu; \\ D_\mu &= \partial_\mu - ig_2\left(\frac{\tau^i}{2}W_\mu^i\right); \\ D_\mu &= \partial_\mu - ig_3\left(\frac{\lambda^a}{2}G_\mu^a\right); \end{aligned}$$

| Boson     | Tensor         | Coupling constant | Physical sate      | $SU(3)_C \otimes SU(2)_L \otimes U(1)_Y$ |
|-----------|----------------|-------------------|--------------------|--|
| $B_\mu$   | $B_{\mu\nu}$   | $g_1 = e$         | photon, Z          | (1,1,0)                                  |
| $W_\mu^i$ | $W_{\mu\nu}^i$ | $g_2$             | $\gamma, W^+, W^-$ | (1,3,0)                                  |
| $G_\mu^a$ | $G_{\mu\nu}^a$ | $g_3$             | gluons             | (8,1,0)                                  |

Table 2.1: The Standard Model Bosons

## 2.2.2 Fermionic Field in SM

Fermions have three generations. A charged lepton, neutrino and up and down type quarks belong to each generation. Furthermore, they are split into left and right fermions. Left handed fermions are doublet under  $SU(2)_L$  while right handed are singlet under  $SU(2)_L$  as shown in Table2.2.

The fermionic field of SM explained by Dirac Lagrangian

$$\mathcal{L} = \bar{\psi}i\gamma_\mu\partial^\mu\psi - m\bar{\psi}\psi$$

as

$$\psi = \begin{pmatrix} \psi_L \\ \psi_R \end{pmatrix}$$

Where as  $\psi_L$  and  $\psi_R$  are left and right handed Spinors respectively. The Gell-Mann-Nishijima formula is defined as

$$Q = I_3 + \frac{Y}{2}$$

The  $Q, I_3$  and  $Y$  denotes the charge, isospin and hypercharge respectively  
The fermionic field Lagrangian is written as

$$\mathcal{L}_{fermion} = i\bar{l}_L \not{D}_L l_L + i\bar{q}_L \not{D}_Q q_L + i\bar{e}_R \not{D}_e e_R + i\bar{u}_R \not{D}_u u_R + i\bar{d}_R \not{D}_d d_R \quad (2.7)$$

Where  $\not{D} = \gamma^\mu D_\mu$

$$\begin{aligned} D_l^\mu &= \partial_\mu - ig_1 Y_l B^\mu - ig_2 \sigma^i W^{i,\mu} \\ D_{q_L}^\mu &= \partial_\mu - ig_1 Y_{q_L} B^\mu - ig_2 \sigma^i W^{i,\mu} - ig_3 t^a G^{a,\mu} \\ D_e^\mu &= \partial_\mu - ig_1 Y_e B^\mu \\ D_{q_R}^\mu &= \partial_\mu - ig_1 Y_{q_R} B^\mu - ig_3 t^a G^{a,\mu} \quad q_R = u_R, d_R \end{aligned}$$

Here  $\sigma^i = \frac{\tau^i}{2}$  belongs to pauli matrices are generator of  $SU(2)$ ,  $t^a = \frac{\lambda^a}{2}$  belongs to Gell-Mann matrices are generator of  $SU(3)$ .

So

$$\begin{aligned} \mathcal{L}_{fermion} &= i\bar{l}_L \gamma^\mu \left( \partial_\mu + ig_1 B_\mu \left(-\frac{1}{2}\right) + ig_2 W_\mu^i \frac{\tau^i}{2} \right) l_L \\ &+ i\bar{q}_L \gamma^\mu \left( \partial_\mu + ig_1 B_\mu \left(\frac{1}{6}\right) + ig_2 W_\mu^i \frac{\tau^i}{2} + ig_3 G_\mu^a \frac{\lambda^a}{2} \right) q_L \\ &+ i\bar{e}_R \gamma^\mu \left( \partial_\mu + ig_1 B_\mu \left(-\frac{2}{3}\right) \right) e_R \\ &+ i\bar{u}_R \gamma^\mu \left( \partial_\mu + ig_1 B_\mu \left(\frac{2}{3}\right) + ig_3 G_\mu^a \frac{\lambda^a}{2} \right) u_R \\ &+ i\bar{d}_R \gamma^\mu \left( \partial_\mu + ig_1 B_\mu \left(-\frac{1}{3}\right) + ig_3 G_\mu^a \frac{\lambda^a}{2} \right) d_R \end{aligned}$$

| Notation | $I_3$                                       | Y              | Q   | Contents  | $SU(3)_c \otimes SU(2)_L \otimes U(1)_Y$ |
|----------|---|----------------|---|---|--|
| $l_L$    | $\begin{pmatrix} 1/2 \\ -1/2 \end{pmatrix}$ | -1             | $\begin{pmatrix} 0 \\ -1 \end{pmatrix}$     | $\begin{pmatrix} \nu_{eL} \\ e_L \end{pmatrix} \begin{pmatrix} \nu_{\mu L} \\ \mu_L \end{pmatrix} \begin{pmatrix} \nu_{\tau L} \\ \tau_L \end{pmatrix}$ | $(1, 2, \frac{-1}{2})$                   |
| $q_L$    | $\begin{pmatrix} 1/2 \\ -1/2 \end{pmatrix}$ | $\frac{1}{3}$  | $\begin{pmatrix} 2/3 \\ -1/3 \end{pmatrix}$ | $\begin{pmatrix} u_L \\ d_L \end{pmatrix} \begin{pmatrix} c_L \\ s_L \end{pmatrix} \begin{pmatrix} t_L \\ b_L \end{pmatrix}$                            | $(3, 2, \frac{1}{6})$                    |
| $e_R$    | 0   | -2             | -1  | $e_R \quad \mu_R \quad \tau_R$  | $(1, 1, 1)$                              |
| $u_R$    | 0   | $\frac{4}{3}$  | $\frac{2}{3}$                               | $u_R \quad c_R \quad t_R$   | $(\bar{3}, 1, \frac{-2}{3})$             |
| $d_R$    | 0   | $\frac{-2}{3}$ | $\frac{-1}{3}$                              | $d_R \quad s_R \quad b_R$   | $(\bar{3}, 1, \frac{1}{3})$              |

Table 2.2: Standard Model fermions

## Charged Current

According to weak interaction theory the weak interactions only exist on left quark's and lepton's doublet.

$$\begin{aligned} \mathcal{L}_{fermions} &= i(\bar{u}_L, \bar{d}_L) \gamma_\mu (\partial^\mu - \frac{1}{2} ig W_i^\mu \tau_i) \begin{pmatrix} u_L \\ d_L \end{pmatrix} \\ &= i\bar{u}_L \gamma_\mu \partial^\mu u_L + i\bar{d}_L \gamma_\mu \partial^\mu d_L - \frac{1}{2} g \bar{u}_L \gamma_\mu W^{-\mu} d_L - \frac{1}{2} g \bar{d}_L \gamma_\mu W^{+\mu} u_L \end{aligned}$$



The pauli matrices ( $i = 1, 2$ ) are used.  $W^\pm$  gauge boson are responsible for flavor changing from up to down and down to up as well. These kind of interactions are called charge current.

$$\mathcal{L}_{CC} = -\frac{1}{2}g\bar{u}_L\gamma_\mu W^{-\mu}d_L - \frac{1}{2}g\bar{d}_L\gamma_\mu W^{+\mu}u_L \quad (2.8)$$

### 2.2.3 Higgs Lagrangian

The Higgs sector be explained by introducing a new complex scalar doublet  $\phi$ .

$$\phi = \begin{pmatrix} \phi_+ \\ \phi_0 \end{pmatrix}$$

it transform as

$$\begin{pmatrix} SU(3)_c & SU(2)_L & U(1)_Y \\ 1 & 2 & \frac{1}{2} \end{pmatrix}$$

The scalar doublet embedded in the Lagrangian as

$$\mathcal{L}_{Higgs} = |(\partial_\mu + ig_1 B_\mu(\frac{1}{2}) + ig_2 W_\mu^i \frac{\tau^i}{2})\phi|^2 - \frac{m^2}{2}|\phi|^2 - \frac{\lambda}{4}|\phi|^4 \quad (2.9)$$

### 2.2.4 Higgs Mechanism

Higgs mechanism [13]is an interesting phenomena that explains how to give masses to gauge bosons and fermions in the Standard Model(SM). Higgs mechanism is utilized to get rid of the Goldstone theorem. According to this condition, Lagrangian is invariant under local transformation.

$$\phi(y) \longrightarrow \phi'(y) = e^{ig\alpha(y)}\phi(y), \quad \phi^*(y) \longrightarrow \phi'^*(y) = e^{-ig\alpha(y)}\phi^*(y)$$

The Lagrangian is

$$\mathcal{L} = (D_\mu\phi)^\dagger(D^\mu\phi) + m^2\phi^\dagger\phi - \lambda(\phi^\dagger\phi)^2 - \frac{1}{4}F_{\mu\nu}F^{\mu\nu} \quad (2.10)$$

where  $A_\mu$  is defined as massless gauge boson field,  $m$  and  $\lambda > 0$  are real parameters,  $F_{\mu\nu} = \partial_\mu A_\nu - \partial_\nu A_\mu$ ,  $\phi$  denote as complex scalar field.

Replacing  $\partial_\mu$  by  $\mathcal{D}_\mu$

$$\partial_\mu\phi \longrightarrow D_\mu\phi, \quad \partial_\mu\phi^\dagger \longrightarrow (D_\mu\phi)^\dagger$$

where,

$$\mathcal{D}_\mu = \partial_\mu + igA_\mu$$

and

$$A_\mu \longrightarrow A_\mu - \partial_\mu \alpha.$$

Considering  $\alpha(x) = \frac{\eta(x)}{V}$ , the gauge transform as

$$\begin{aligned}\phi &\longrightarrow \phi' = e^{ig\frac{\eta}{V}} \phi \\ A_\mu &\longrightarrow A_\mu - \partial_\mu \eta\end{aligned}$$

Applying these transformation the  $\mathcal{L}$  (2.10) remains same. We use  $\phi(x) = \frac{V+h(x)}{\sqrt{2}}$  in Eq(2.10), we obtain the expression

$$\begin{aligned}\mathcal{L} = & \frac{1}{2}[(\partial_\mu - igA_\mu)(V+h)(\partial^\mu + igA^\mu)(V+h)] + \frac{1}{2}m^2(V+h)^2 - \frac{1}{4}\lambda(V+h)^4 \\ & - \frac{1}{4}F_{\mu\nu}F^{\mu\nu}\end{aligned}\tag{2.11}$$

The interaction terms in the Lagrangian(2.11) are  $h^3, h^4, hAA$  and  $h^2AA$ . The quadratic terms in the Lagrangian correspond to the mass terms i-e ( $\frac{g^2V^2}{2}A_\mu A^\mu$ ) and  $(-\lambda Vh^2)$  that refer to the gauge boson and scalar boson mass respectively. The gauge boson  $A_\mu$  eats up the Goldstone boson and gives it a mass.

## 2.2.5 Higgs and Yukawa Terms

The dynamic of a spin-0 scalar field can be explained through Higgs part.

$$\mathcal{L}_{higgs} = (D^\mu \phi)^\dagger D_\mu \phi - V(\phi)$$

The potential is

$$V(\phi) = m^2 \phi^\dagger \phi + \lambda (\phi^\dagger \phi)^2$$

Where  $\phi$  is a field defined as an isospin doublet

$$\phi = \begin{pmatrix} \phi^+ \\ \phi^0 \end{pmatrix}\tag{2.12}$$

This field  $\phi$  couples the Higgs boson with the fermion fields using Yukawa coupling. We can further expand the lagrangian by the coupling between the fermion doublets and field  $\phi$  to introduce mass terms for the fermions. This rise the new terms, known as Yukawa interactions, preserved by symmetries. The Yukawa terms Lagrangian is given as

$$\begin{aligned}\mathcal{L}_{yukawa} &= \bar{\psi}_L Y \phi \psi_R + h.c \\ \mathcal{L}_{yukawa} &= Y_u \bar{q}_L \phi u_R + Y_d \bar{q}_L \tilde{\phi} d_R + Y_L \bar{l}_L \tilde{\phi} e_R + h.c\end{aligned}\tag{2.13}$$

$Q_L$  and  $L_L$  are defined as left handed quarks and leptons respectively.

$$l_L = P_L \begin{pmatrix} \nu_e \\ e \end{pmatrix}, \quad q_L = P_L \begin{pmatrix} u \\ d \end{pmatrix}$$

$u_R, d_R$  and  $e_R$  are right handed up-type, down-type quarks and lepton respectively.  
 $u_R = P_R u, \quad d_R = P_R d, \quad e_R = P_R e$   
where

$$P_L = \frac{(1 - \gamma_5)}{2}, \quad P_R = \frac{(1 + \gamma_5)}{2}$$

$Y_u, Y_d,$  and  $Y_L$  are Yukawa couplings for up-type, down-type quarks and lepton respectively. The Yukawa coupling  $Y_q$  where ( $q = u, d, l$ ) are  $3 \times 3$  matrices. Local symmetry breaking can be achieved by substituting various value for  $\phi$  field in Eq(2.12).

$$\phi = \begin{pmatrix} \phi^+ \\ \phi^0 \end{pmatrix} \longrightarrow \frac{1}{\sqrt{2}} \begin{pmatrix} 0 \\ V + h(x) \end{pmatrix} \quad (2.14)$$

The vacuum expectation value (VEV) is not zero and expected at  $\frac{V}{\sqrt{2}}$ , where  $h(x)$  is a perturbation around new VEV represented as the Higgs boson. The Yukawa terms in  $\mathcal{L}$  will be

$$\mathcal{L}_{yukawa} = \frac{V}{\sqrt{2}} \bar{u}_L Y_u u_R + \frac{V}{\sqrt{2}} \bar{d}_L Y_d d_R + \frac{V}{\sqrt{2}} \bar{e}_L Y_L e_R + h.c \quad (2.15)$$

## 2.3 CKM matrix and Fermion masses

The masses of gauge boson  $W^\pm$  and  $Z$  gets through the SSB of the gauge group  $SU(2)_L \otimes U(1)_Y$ . Why flavor changing neutral current is not allow at tree level in SM? How we can generate fermions masses? We desperately required a term that couple the fermions with Higgs doublet. They must be gauge invariant and renormalizable. These terms are called Yukawa terms in the Lagrangian. The Lagrangian for the charge lepton corresponding to first generation is

$$\mathcal{L}_{Yukawa,1}^{Leptons} = -Y_e \bar{e}' \phi^\dagger \begin{pmatrix} e \\ \nu_e \end{pmatrix}'_L + h.c. \quad (2.16)$$

For the three generations, the Lagrangian is written in the generalized form as

$$\mathcal{L}_{Yukawa}^{Leptons} = -(\bar{e}'_R \quad \bar{\mu}'_R \quad \bar{\tau}) Y_l \begin{pmatrix} \phi^\dagger \begin{pmatrix} e \\ \nu_e \end{pmatrix}'_L \\ \phi^\dagger \begin{pmatrix} \mu \\ \nu_\mu \end{pmatrix}'_L \\ \phi^\dagger \begin{pmatrix} \tau \\ \nu_\tau \end{pmatrix}'_L \end{pmatrix} + h.c. \quad (2.17)$$

According to Eq.(2.14) after giving VEV the  $\mathcal{L}_{Yukawa}^{Leptons}$  splits into two parts. One part explains the interaction of leptons with physical Higgs and other part is explained by

$$\mathcal{L}_{Mass}^{Leptons} = -(\bar{e}'_R \quad \bar{\mu}'_R \quad \bar{\tau}) M_l \begin{pmatrix} e \\ \mu \\ \tau \end{pmatrix}'_L \quad (2.18)$$

where,

$$M_l = \frac{V}{\sqrt{2}} Y_l$$

In principle  $M_l$  is an arbitrary 3 complex matrix and cannot be named as mass matrix. However the charge lepton fields are possible to transform in such fashion that  $M_l$  is defined as diagonal matrix with positive real or zero number elements. The Lagrangian derived by applying this type of transformation to all of its term will latter be expressed as the mass eigenstate of the leptons. The new Lagrangian of charge current carries flavor mixing term. All lepton fields now taking place are mass eigenstate, for distiction we use without prime notation.

To analyze the quarks masses  $d$ ,  $s$  and  $b$  are the down type quark masses, the Yukawa Lagrangian is same as the one in Eq.(2.17) with  $Y_q^d$  Yukawa matrix. The up-type quark is a bit different, we replace  $\phi$  with  $i\sigma_2\phi^*$  as the  $SU(2)_L$  doublet. Where  $\sigma_2$  is the pauli matrix

$$\mathcal{L}_{Yukawa}^{U-quarks} = -(\bar{u}'_R \quad \bar{c}'_R \quad \bar{t}'_R) Y_q^u \begin{pmatrix} i\sigma_2\phi^* \begin{pmatrix} u \\ d \end{pmatrix}'_L \\ i\sigma_2\phi^* \begin{pmatrix} c \\ s \end{pmatrix}'_L \\ i\sigma_2\phi^* \begin{pmatrix} t \\ b \end{pmatrix}'_L \end{pmatrix} + h.c. \quad (2.19)$$

The Yukawa matrices are diagonalized by using the unitary transformation of the quark fields explicitly it is given as below

$$\begin{pmatrix} u \\ c \\ t \end{pmatrix}'_L = V_u \begin{pmatrix} u \\ c \\ t \end{pmatrix}_L, \quad \begin{pmatrix} u \\ c \\ t \end{pmatrix}'_R = U_u \begin{pmatrix} u \\ c \\ t \end{pmatrix}_R$$

$$\begin{pmatrix} d \\ s \\ b \end{pmatrix}'_L = V_d \begin{pmatrix} d \\ s \\ b \end{pmatrix}_L, \quad \begin{pmatrix} d \\ s \\ b \end{pmatrix}'_R = U_d \begin{pmatrix} d \\ s \\ b \end{pmatrix}_R. \quad (2.20)$$

Where  $V_u$ ,  $U_u$ ,  $V_d$ ,  $U_d$  belong to  $U(3)$ . In the lepton sector only one set exist like these matrices, which diagonalize the yukawa matrices and that is the reason behind the Lagrangian having different mass eigenstates from the weak eigenstate. The quarks mixing in different

generation is defined by the CKM matrix known as Cabibbo-Kobayashi-Maskawa matrix which relates weak eigenstates with mass eigenstates.

$$V_{CKM} = V_u^\dagger V_d.$$

We can introduce these quarks coupling terms with  $W^\pm$  bosons

$$\mathcal{L}_{CC}^{Quarks} = -\frac{e}{2 \sin \theta_W} (W_\mu^+ J^{\mu,-} + W_\mu^- J^{\mu,+}) \quad (2.21)$$

Where,

$$J^{\mu,-} = (\bar{u} \quad \bar{c} \quad \bar{t})_L V_{CKM} \begin{pmatrix} d \\ s \\ b \end{pmatrix}_L \quad (2.22)$$

In  $\mathcal{L}(2.8)$  for the Charge current will become

$$\begin{aligned} \mathcal{L}_{CC} &= -\frac{1}{2} g \bar{u}_L \gamma_\mu W^{-\mu} d_L - \frac{1}{2} g \bar{d}_L \gamma_\mu W^{+\mu} u_L \\ &= -\frac{1}{2} g \bar{u}_L V_L^{u\dagger} V_L^d \gamma_\mu W^{-\mu} d_L - \frac{1}{2} g \bar{d}_L V_L^{d\dagger} V_L^u \gamma_\mu W^{+\mu} u_L \end{aligned} \quad (2.23)$$

The  $V_L^{u\dagger} V_L^d$  matrix product consisting of off-diagonal terms causes the transition of coupling of quarks from one doublet to the other doublets involving weak transition and charged current. This phenomena is called quark mixing and  $d'_L$  defined for down type quarks consists of mixed quark mass states.

$$d'_L = \begin{pmatrix} d' \\ s' \\ b' \end{pmatrix} = V_L^{u\dagger} V_L^d d_L = \begin{pmatrix} V_{ud} & V_{us} & V_{ub} \\ V_{cd} & V_{cs} & V_{cb} \\ V_{td} & V_{ts} & V_{tb} \end{pmatrix} \begin{pmatrix} d \\ s \\ b \end{pmatrix} \quad (2.24)$$

For instance the first element  $d'$  is the superposition mass state of  $d, s$  and  $b$  that depends on  $V_{ud}, V_{us}$  and  $V_{ub}$ . The  $V_L^{u\dagger} V_L^d$  matrix product is called CKM matrix [8]. The components are calculated by experimental analysis [14].

$$\begin{pmatrix} |V_{ud}| \approx 0.974 & |V_{us}| \approx 0.25 & |V_{ub}| \approx 0.003 \\ |V_{cd}| \approx 0.225 & |V_{cs}| \approx 0.973 & |V_{cb}| \approx 0.04 \\ |V_{td}| \approx 0.009 & |V_{ts}| \approx 0.040 & |V_{tb}| \approx 0.999 \end{pmatrix} \quad (2.25)$$

The CKM matrix explain in the following standard parametrization as [14]

$$\mathbf{V}_{CKM} = \begin{pmatrix} V_{ud} & V_{us} & V_{ub} \\ V_{cd} & V_{cs} & V_{cb} \\ V_{td} & V_{ts} & V_{tb} \end{pmatrix} \quad (2.26)$$

$$= \begin{pmatrix} C_{12}C_{13} & S_{12}S_{13} & S_{13}e^{-i\Delta} \\ -S_{12}C_{23} - C_{12}S_{23}S_{13}e^{i\Delta} & C_{12}S_{23} - S_{12}S_{23}S_{13}e^{i\Delta} & S_{23}C_{13} \\ S_{12}C_{23} - C_{12}S_{23}S_{13}e^{i\Delta} & -S_{23}C_{12} - S_{12}C_{23}S_{13}e^{i\Delta} & C_{23}C_{13} \end{pmatrix} \quad (2.27)$$

Here  $C_{ab} = \cos\theta_{ab}$ ,  $S_{ab} = \sin\theta_{ab}$  ( $a, b = 1, 2, 3$ ) and  $\Delta$  is the phase with the range  $0 \leq \Delta \leq 2\pi$ .  $S_{12} = |V_{us}|$ ,  $S_{13} = |V_{ub}|$ ,  $S_{23} = |V_{cb}|$  and  $\Delta$ .  $S_{12}$ ,  $S_{13}$  and  $S_{23}$  are four independent parameter which is obtained by tree-level decays. Numerical calculations can be done suitably by standard parametrization.

# Theoretical Framework for $B$ Meson Decay

In this chapter we will present the theoretical framework for rare  $B$  meson decays which is based on the effective field theory. The formalism of effective field theory can be used to describe the weak decays. Furthermore we also briefly discuss the new physics scenarios such as model independent/ leptoquark model and  $Z'$  models. The phenomenology of these models is discussed in chapter 4.

## 3.1 Effective Field Theory

Effective field theory (EFT) [15,16] is one of the ingredients in quantum field theory which will be used to analyze the multiscale problems. Consider a field theory whose characteristic energy scale  $\kappa$ , and suppose that we want to discuss physics at some much lower scale  $E \ll \kappa$ . To build such EFT one chooses a cutoff scale, which is slightly less than the energy scale and integrates out the heavy degrees of freedom. In general, the effective Lagrangian is written as;

$$\mathcal{L}_{eff} = \sum_{n \geq 0} C_n(\mu) O_n \quad (3.1)$$

The Lagrangian is an infinite sum over the operators  $O_n$ , where  $C_n(\mu)$  is the coupling constant known as Wilson coefficients. So one can ask about the predictability of this theory. The answer to the above question is by substituting the coupling constant  $C_n(\mu)$  with a dimensionless constant  $c_{i_n}$ . So the new form of the Lagrangian is

$$\mathcal{L}_{eff} = \mathcal{L}^0 + \sum_{n > 0} \sum_{c_{i_n}} \frac{c_{i_n}}{\kappa^n} O_{i_n} \quad (3.2)$$

The higher dimension operators are suppressed with the increasing power of  $\kappa$ . The lowest dimensional operators are more important due to which one can cut off the series and only

the finite couplings and number of operator will remain.

The lowest dimensional operator will be more important. However it depends on the precision goal, where one can terminate the series and only the finite number of operators and couplings should preserved

### 3.1.1 Operator Product Expansion

Operator product expansion (OPE) is one of the important tool to investigate the weak interaction of quarks. To illustrate the phenomenon of OPE, consider a weak decay of hadron  $D^0 \rightarrow K^- \pi^+$  which at quark level occurs at  $c \rightarrow s u \bar{d}$  as shown in the fig.(3.1). The full amplitude of such decay can be written by using Feynman rules for weak interaction process and can be expressed as,

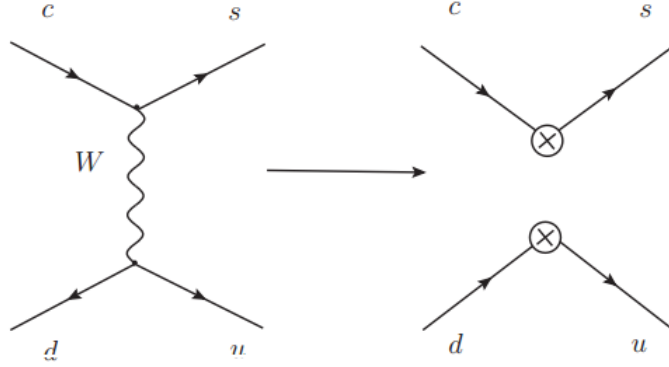


Figure 3.1: Left shows full theory and at Right the effective theory in  $c \rightarrow s u \bar{d}$

$$\begin{aligned} \mathcal{M}_{Full} &= \frac{g_2^2}{8} V_{cs}^* V_{ud} [\bar{u}_s(p_s) \gamma_\mu (1 - \gamma_5) u_c(p_c)] \frac{g^{\mu\nu}}{k^2 - m_w^2} [\bar{u}_u(p_u) \gamma_\nu (1 - \gamma_5) u_d(p_d)] \\ \mathcal{M}_{Full} &= \frac{G_F}{\sqrt{2}} V_{cs}^* V_{ud} [\bar{u}_s(p_s) \gamma_\mu (1 - \gamma_5) u_c(p_c)] \frac{m_w^2}{k^2 - m_w^2} [\bar{u}_u(p_u) \gamma^\mu (1 - \gamma_5) u_d(p_d)] \quad (3.3) \end{aligned}$$

$G_F$  is Fermi constant

$$\frac{G_F}{\sqrt{2}} = \frac{g_2^2}{8m_w^2} \quad (3.4)$$

Expanding the amplitude to  $O(\frac{k^2}{m_w^2})$

$$\mathcal{M}_{Full} = -\frac{G_F}{\sqrt{2}} V_{cs}^* V_{ud} [\bar{u}_s(p_s) \gamma_\mu (1 - \gamma_5) u_c(p_c)] [\bar{u}_u(p_u) \gamma^\mu (1 - \gamma_5) u_d(p_d)] + O(\frac{k^2}{m_w^2}) \quad (3.5)$$

Where  $k$  is the momentum transferred due to  $W$  propagator and its value is small as compared to  $m_w$ . We can neglect the terms  $O(\frac{k^2}{m_w^2})$  without any hesitation from Eq(3.5). Now the full amplitude will be approximately equal to

$$\mathcal{M}_{Full} \approx -\frac{G_F}{\sqrt{2}} V_{cs}^* V_{ud} [\bar{u}_s(p_s) \gamma_\mu (1 - \gamma_5) u_c(p_c)] [\bar{u}_u(p_u) \gamma^\mu (1 - \gamma_5) u_d(p_d)] \quad (3.6)$$



The same result is obtained by the effective Hamiltonian

$$\mathcal{H}_{eff} = \frac{G_F}{\sqrt{2}} V_{cs}^* V_{ud} [\bar{s}\gamma_\mu(1 - \gamma_5)c][\bar{u}\gamma^\mu(1 - \gamma_5)d] + \text{higher Dim operator} \quad (3.7)$$

where

$$Q = [\bar{s}\gamma_\mu(1 - \gamma_5)c][\bar{u}\gamma^\mu(1 - \gamma_5)d]$$

In this example the value of Wilson coefficient  $C_i(\mu) = 1$ . This corresponds to the low energy scale, where the heavier particles momenta is integrated out and the higher dimension operator represented by the terms of order  $O(\frac{k^2}{m_w^2})$ . The OPE idea is grasped through above example. The significant property of OPE is to separate physics into two regime i-e the low and high energy regime.

In this way the effective Hamiltonian is defined as the linear combination of these operators. From the matching condition  $\mathcal{M}_{full} = \mathcal{M}_{eff}$  amplitude we get the Wilson coefficient  $C_i(\mu)$

$$\mathcal{M}_{full} = \mathcal{M}_{eff} = \frac{G_F}{\sqrt{2}} \sum_i V_{CKM}^i C_i(\mu) \langle O_i(\mu) \rangle \quad (3.8)$$

$\langle O_i(\mu) \rangle$  bracket denoted matrix element to the relevant operator  $O_i(\mu)$ . This is called the matching condition of the full theory with effective theory. The full theory deals with the particles having dynamical degree of freedom while in effective theory we integrate out the heavy degree of freedom.

## 3.2 Effective Hamiltonian

The phenomenology of B-decays can be described by effective Hamiltonian. As mentioned in chapter 1, the decay under consideration is  $B_c \rightarrow D_s^* \ell^+ \ell^-$ , at quark level this decay is governed by the transition  $b \rightarrow s \ell^+ \ell^-$  hence the effective Hamiltonian for such decay can be expressed as

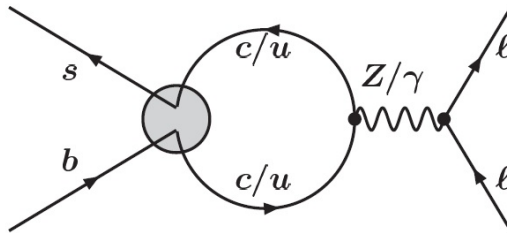


Figure 3.2: Effective diagram of  $b \rightarrow s \ell^+ \ell^-$

$$\mathcal{H}_{eff} = -\frac{G_F V_{ts}^* V_{tb}}{\sqrt{2}} \sum_{i=1} C_i(\mu) Q_i(\mu) \quad (3.9)$$

Now we write amplitude, the initial state of meson  $B_c$  goes into  $D_s^*$  which is final state meson, can be written as

$$\mathcal{M}(B_c \rightarrow D_s^*) = \langle D_s^* | H_{eff} | B_c \rangle \quad (3.10)$$

$$= -\frac{G_F V_{ts}^* V_{tb}}{\sqrt{2}} \sum_{i=1}^{10} C_i(\mu) \langle D_s^* | Q_i(\mu) | B_c \rangle \quad (3.11)$$

Where  $V_{ts}^* V_{tb}$  are CKM matrix elements,  $Q_i(\mu)$  are local quark operators and  $C_i(\mu)$  are Wilson coefficients. The high energy physics are encoded in the WC's  $C_i(\mu)$  and low energy physics are hidden in the local quark operators. The explicit form of these local quark operators are given as follows [17];

### Current-Current Operator

$$\begin{aligned} Q_1 &= (\bar{s}_i c_j)_{V-A} (\bar{c}_j b_i)_{V-A}, \\ Q_2 &= (\bar{s} c)_{V-A} (\bar{c} b)_{V-A}, \end{aligned}$$

### Quantum Chromodynamics Penguin Operator

$$\begin{aligned} Q_3 &= (\bar{s} b)_{V-A} \sum_q (\bar{q} q)_{V-A}, \\ Q_4 &= (\bar{s}_i b_j)_{V-A} \sum_q (\bar{q}_j q_i)_{V-A}, \\ Q_5 &= (\bar{s} b)_{V-A} \sum_q (\bar{q} q)_{V+A}, \\ Q_6 &= (\bar{s}_i b_j)_{V-A} \sum_q (\bar{q}_j q_i)_{V+A}, \end{aligned}$$

where  $q=u, d, b, s, c$

### Magnetic Dipole Operator

$$\begin{aligned} Q_7 &= \frac{e}{8\pi^2} m_b (\bar{s} \sigma^{\mu\nu} (1 + \gamma_5) b) F_{\mu\nu}, \\ Q_8 &= \frac{e}{8\pi^2} m_b (\bar{s}_i \sigma^{\mu\nu} (1 + \gamma_5) T_{ij} b_j) G_{\mu\nu}, \end{aligned}$$

### Semileptonic electroweak penguin operator

$$\begin{aligned}
Q_9 &= \frac{e}{8\pi^2}(\bar{s}b)_{V-A}(\bar{l}l)_V, \\
Q_{10} &= \frac{e}{8\pi^2}(\bar{s}b)_{V-A}(\bar{l}l)_A.
\end{aligned} \tag{3.12}$$

where  $(V\pm A)$  stands for  $\gamma^\mu(1\pm\gamma^5)$ . Gluon and photon field are the  $G_{\mu\nu}$  and  $F_{\mu\nu}$  respectively;  $T_{ij}$  represents the generators of the SU(3) color group;  $i$  and  $j$  are color indices.

In rare B meson decays, several decay modes precisely discussed in literature such as  $B \rightarrow X_s \ell^+ \ell^-$ ,  $B \rightarrow (K, K^*) \ell^+ \ell^-$  [7, 18, 19] based on quark level transitions  $b \rightarrow s \ell^+ \ell^-$  mediated via FCNC at loop level in SM. Many models are proposed in literature such as  $Z'$  models, Leptoquarks, SUSY and Universal extra dimension (UED) model which are powerful tool to search NP in said decays.

In this thesis, we consider only those NP models where the effects of NP can be observed only through the modification of WC's.

## New Physics Models

To investigate the NP effects via  $B_c \rightarrow D_s^* \ell^+ \ell^-$  decays, we consider two different NP models such as heavy and light  $Z'$  models, Model independent/leptoquark models.

### 3.3 Model Independent Scenarios

In model independent scenarios all possible contributions in the form of Wilson coefficient and operators are taken into account in effective Hamiltonian. We write effective Hamiltonian for quark level transition  $b \rightarrow s \mu^+ \mu^-$

$$\mathcal{H}_{eff} = -\frac{G_F V_{ts}^* V_{tb} \alpha}{\sqrt{2}\pi} \sum_{k=9,10} (C_k Q_k + C'_k Q'_k) \tag{3.13}$$

$$\begin{aligned}
Q_9 &= [\bar{s}\gamma_\mu P_L b][\bar{\mu}\gamma^\mu \mu] \\
Q_{10} &= [\bar{s}\gamma_\mu P_L b][\bar{\mu}\gamma^\mu \gamma_5 \mu]
\end{aligned} \tag{3.14}$$

Where we can get prime operators by replacing  $P_L \rightarrow P_R$  and primed wilson coefficient have contributions from both SM and NP. There are a number of observables and experimental measurements can be used to constraint on NP for transition  $b \rightarrow s \mu^+ \mu^-$  to get new physics wilson coefficient.

There are three different NP scenarios discussed in literature [20];

- (I)  $C_9^{\mu\mu}(NP) < 0$

- (II)  $C_9^{\mu\mu}(NP) = -C_{10}^{\mu\mu}(NP) < 0$
- (III)  $C_9^{\mu\mu}(NP) = C_9^{\mu\mu'}(NP) < 0$

Scenarios (I) and (II) will be taken to search the effects of NP in MI scenarios [20]. However, scenario (III) is ignored because it disagreed with experimental measurement. Leptoquark model could be only taken for scenario II. However,  $Z'$  models could be taken for both scenarios. we add model independent NP wilson coefficient  $C_9(NP)$  and  $C_{10}(NP)$  in the SM WC's  $C_9(SM)$  and  $C_{10}(SM)$  to search NP effects in said decay.

Here, we use two types of data fit for this transition  $b \rightarrow s\mu^+\mu^-$ , we analyze only CP conserving observables in fit A and we study  $R_{K^*}$  in fit B [1]. Fit-A and fit-B are taken in both the model dependent and MI analysis. The values of these WC's couplings of fit A and fit B taken from ref. [1] are given in table 3.1.

| Scenarios                                      | fit-A            | fit-B            |
|--|------------------|------------------|
| (I) $C_9^{\mu\mu}(NP)$                         | $-1.20 \pm 0.20$ | $-1.25 \pm 0.19$ |
| (II) $C_9^{\mu\mu}(NP) = -C_{10}^{\mu\mu}(NP)$ | $-0.62 \pm 0.14$ | $-1.68 \pm 0.12$ |
| (III) $C_9^{\mu\mu}(NP) = -C_9^{\mu\mu'}(NP)$  | $-1.10 \pm 0.18$ | $-1.11 \pm 0.17$ |

Table 3.1: MI scenarios: WCs values in best fitting are taken from ref. [1]

### 3.3.1 Leptoquark Model

It is well known that Leptoquarks are spin-0 scalar or spin-1 vector bosonic particles that can couple to a lepton and a quark at the same time. The Leptoquark (LQ) models were explained in Ref. [20,21]. There are only three from the ten, LQ Models which could couple with SM particles having dimension less than or equal to 4 operators, explain  $b \rightarrow s\mu^+\mu^-$ . We consider here scalar isotriplet Leptoquarks( $S_3$ ) which potentially contribute to the  $b \rightarrow s\mu^+\mu^-$  transition. The LQs transform as like SM guage symmetry  $SU(3) \otimes SU(2) \otimes U(1)$ . After integrating out the heavy scalar LQ boson, effective Hamiltonian of Heavy LQ model can be written as [21]

$$\mathcal{H}_{eff} = -\frac{G_F V_{ts}^* V_{tb} \alpha}{\sqrt{2}\pi} (C_9^{NP} Q'_9 + C_{10}^{NP} Q'_{10}) \quad (3.15)$$

All LQ models associated with only scenario (II).  $C_9^{\mu\mu}(NP) = -C_{10}^{\mu\mu}(NP)$ .

$$\mathcal{H}_{eff} = -\frac{G_F V_{ts}^* V_{tb} \alpha}{\sqrt{2}\pi} C_9^{NP} (Q'_9 - Q'_{10}) \quad (3.16)$$

We will obtain  $Q'_9, Q'_{10}$  by flipping the projection operator  $P_L \rightarrow P_R$  in  $Q_9, Q_{10}$  from eq.3.12. The WC's of LQ Model is directly proportional to fermions coupling  $g_L^{b\mu} g_L^{s\mu}$  is given in ref. [20]

$$C_9^{\mu\mu}(NP) \propto \frac{g_L^{b\mu} g_L^{s\mu}}{M_{LQ}^2} \quad (3.17)$$

couplings of LQ are  $g_L^{b\mu} g_L^{s\mu}$  and  $M_{LQ}$  is the leptoquark mass. The value of WC's is same as for Model Independent fit, given in table 3.1.

### 3.3.2 $Z'$ Model

The  $Z'$  model [22–27] is the extension of SM, addition of an extra  $U(1)'$  gauge symmetry to the SM structure. One extra  $U(1)'$  gauge symmetry associated with a neutral gauge boson  $Z'$  gives off-diagonal couplings of non-universal  $Z'$  with fermions due to this FCNC transitions could occur at tree level in  $Z'$  model [28, 29]. We write the neutral current Lagrangian in the SM with  $Z'$  contribution as [30]

$$\mathcal{L}_{NC} = \mathcal{L}_{SM}^Z - g_2^{Z'} J'_\mu Z'^\mu \quad (3.18)$$

where  $g_2^{Z'}$  is the gauge coupling of  $Z'$  and  $\mathcal{L}_{SM}^Z = -e J_{em}^\mu A_\mu - g_Z J_Z^\mu Z_\mu$ . The  $Z'$  current is given as;

$$J'_\mu = \sum_{i,j} \bar{\Psi}_i \gamma_\mu [(\epsilon_{\Psi L})_{ij} P_L + (\epsilon_{\Psi R})_{ij} P_R] \Psi_j \quad (3.19)$$

where  $\Psi$  denotes weak eigenstates of SM fermions, the sum is over the fermion flavors,  $P_{L,R} \equiv (1 \mp \gamma_5)/2$ , and  $\epsilon_{\Psi L,R}$  denote the chiral couplings.  $Z'$  must transform as a triplet or singlet of  $SU(2)_L$  and couples to left handed quarks. The fermion Yukawa matrices  $\mathcal{Y}_\Psi$  in the weak eigenstate basis are diagonalized by the unitary matrices  $V_{L,R}^\Psi$ ;

$$\mathcal{Y}_\Psi^{diag} = V_R^\Psi \mathcal{Y}_\Psi V_L^{\Psi\dagger} \quad (3.20)$$

Here,  $V_{CKM} = V_R^\Psi V_L^{\Psi\dagger}$

Now, the chiral  $Z'$  couplings in the fermion mass eigenstate basis can be written as;

$$\mathcal{X}^{\Psi L} \equiv V_L^\Psi \epsilon_{\Psi L} V_L^{\Psi\dagger}, \quad \mathcal{X}^{\Psi R} \equiv V_R^\Psi \epsilon_{\Psi R} V_R^{\Psi\dagger} \quad (3.21)$$

Therefore, the chiral  $Z'$  couplings are induced by fermion mixing. Hence, FCNC occur at tree level in  $Z'$  model due to off diagonal coupling of non universal  $Z'$ .

$$\mathcal{X}^{\Psi L,R} = \begin{pmatrix} \mathcal{X}_{11}^{\Psi L,R} & 0 & \mathcal{X}_{13}^{\Psi L,R} \\ 0 & \mathcal{X}_{11}^{\Psi L,R} & \mathcal{X}_{23}^{\Psi L,R} \\ \mathcal{X}_{13}^{\Psi L,R*} & \mathcal{X}_{23}^{\Psi L,R*} & \mathcal{X}_{33}^{\Psi L,R} \end{pmatrix} \quad (3.22)$$

We consider two types of  $Z'$  models such as, Heavy and Light  $Z'$  models both are consistent with  $b \rightarrow s\mu^+\mu^-$ .

### 3.3.3 Heavy $Z'$ Model

We have to taken important constraints form other obervables and experimental measurements for transition  $b \rightarrow s\mu^+\mu^-$  to determine the properties of  $Z'$  accordingly, the Lagrangian of  $Z'$  model can be written as;

$$\mathcal{L}_{Z'} = J'_\mu Z' \quad (3.23)$$

$$J^\mu = -g_{LL}^{\mu\mu} \bar{X} \gamma^\mu P_L X + g_R^{\mu\mu} \bar{\mu} \gamma^\mu P_R \mu + g_L^{bs} \bar{\psi}_{q2} \gamma^\mu P_L \psi_{q3} \quad (3.24)$$

so,  $\psi_{qi}$  denote as the quark doublet, and  $X = (\nu_\mu, \mu)^T$ . We integrated out the heavy  $Z'$  gauge boson [1]. Effective lagrangian containing 4-fermion operators written as;

$$\begin{aligned} \mathcal{L}_{Z'}^{eff} = -\frac{1}{2M_{Z'}^2} J_\mu J^\mu = & - \frac{g_L^{bs}}{M_{Z'}^2} (\bar{s} \gamma^\mu (1 - \gamma^5) b) (\bar{\mu} \gamma^\mu (g_L^{\mu\mu} P_L + g_R^{\mu\mu} P_R) \mu) \\ & - \frac{(g_L^{bs})^2}{2M_{Z'}^2} (\bar{s} \gamma^\mu P_L b) (\bar{\gamma}^\mu P_L b) \\ & - \frac{g_L^{\mu\mu}}{M_{Z'}^2} (\bar{\mu} \gamma^\mu (g^{\mu\mu} P_L + g^{\mu\mu} P_R) \mu) (\bar{\nu}_\mu \gamma^\mu P_L \nu_\mu) \end{aligned} \quad (3.25)$$

Here, we consider two scenarios for the phenomenology of  $Z'$  models are;

- Scenario (I)  $g_R^{\mu\mu} = g_L^{\mu\mu}$
- Scenario (II)  $g_R^{\mu\mu} = 0$

The modified Wilson coefficient's in TeV  $Z'$  are given as;

$$C_9^{\mu\mu}(NP) = \left[ \frac{\pi}{\sqrt{2} G_F \alpha V_{tb} V_{ts}^*} \right] \times \frac{g_L^{bs} (g_L^{\mu\mu} + g_R^{\mu\mu})}{M_{Z'}^2} \quad (3.26)$$

$$C_{10}^{\mu\mu}(NP) = - \left[ \frac{\pi}{\sqrt{2} G_F \alpha V_{tb} V_{ts}^*} \right] \times \frac{g_L^{bs} (g_L^{\mu\mu} - g_R^{\mu\mu})}{M_{Z'}^2} \quad (3.27)$$

Following are the couplings of NP Wilson coefficients of Heavy  $Z'$  model.

| $g_L^{\mu\mu}$ | $Z'(I) g_L^{bs}$                | $Z'(II) g_L^{bs}$               |
|----------------|---------------------------------|---------------------------------|
| 0.5            | $(-1.8 \pm 0.3) \times 10^{-3}$ | $(-1.9 \pm 0.4) \times 10^{-3}$ |

Table 3.2: TeV Heavy  $Z'$  model in best fit values of  $a_L^{bs}$  in fit A in Ref. [1]

The four fermion operators required with in the scenarios are as follows;

| $g_L^{\mu\mu}$ | $Z'(I)g_L^{bs}$                 | $Z'(II)g_L^{bs}$                |
|----------------|---------------------------------|---------------------------------|
| 0.5            | $(-1.9 \pm 0.3) \times 10^{-3}$ | $(-2.1 \pm 0.4) \times 10^{-3}$ |

Table 3.3: TeV Heavy  $Z'$  model in best fit values of  $a_L^{bs}$  in fit B in Ref. [1]

- (I)  $[\bar{s}\gamma_\mu P_L b][\bar{\mu}\gamma^\mu \mu]$
- (II)  $[\bar{s}\gamma_\mu P_L b][\bar{\mu}\gamma^\mu P_L \mu]$
- (III)  $[\bar{s}\gamma_\mu \gamma_5 b][\bar{\mu}\gamma^\mu \mu]$

There are two scenarios for  $Z'$  Model. It is natural for  $Z'$  gauge boson to couple vectorially to  $\bar{s}_L b_L$  and  $\bar{\mu}\mu$  or  $\bar{\mu}_L \mu_L$  as scenario (III) have need that  $Z'$  couple axial-vectorially to  $\bar{s}b$  which seems not natural. All things considered, we exclude scenario (III) which has disagreement with experiments.

### 3.3.4 Light $Z'$ Model

In Light  $Z'$  Model, we have two different mass ranges  $m_{Z'} > m_B$  and  $m_{Z'} < 2m_\mu$ , first range have implication in dark matter and second range discuss the muon measurement of  $g-2$  and have application for neutrino interaction. Here, we consider first range for  $m_{Z'} = 10\text{GeV}$ .

The modified Wilson coefficient's for GeV  $Z'$  are given as;

$$C_9^{\mu\mu}(NP) = \left[ \frac{\pi}{\sqrt{2}G_F \alpha V_{tb} V_{ts}^*} \right] \times \frac{(a_L^{bs} + g_L^{bs}(q^2/m_B^2))(g_L^{\mu\mu} + g_R^{\mu\mu})}{q^2 - M_{Z'}^2} \quad (3.28)$$

$$C_{10}^{\mu\mu}(NP) = - \left[ \frac{\pi}{\sqrt{2}G_F \alpha V_{tb} V_{ts}^*} \right] \times \frac{(a_L^{bs} + g_L^{bs}(q^2/m_B^2))(g_L^{\mu\mu} - g_R^{\mu\mu})}{q^2 - M_{Z'}^2} \quad (3.29)$$

Here we have the WC's are  $q^2$  dependent in Light  $Z'$  model for  $b \rightarrow s\mu^+\mu^-$ .

In the GeV Light  $Z'$  model  $a_L^{bs}$  is present, so here we will unconcern  $g_L^{bs}$ . Following are the couplings of NP wilson coefficients of Light  $Z'$  model.

| $g_L^{\mu\mu}$ | $Z'(I) a_L^{bs}$                | $Z'(II) a_L^{bs}$               |
|----------------|---------------------------------|---------------------------------|
| 1.2            | $(-5.2 \pm 1.2) \times 10^{-6}$ | $(-7.2 \pm 1.8) \times 10^{-6}$ |

Table 3.4: GeV Light  $Z'$  model in best fit values of  $a_L^{bs}$  in fit A in Ref. [1]

# Analysis of Decay $B_c \rightarrow D_s^* \ell^+ \ell^-$ Beyond SM

## 4.1 Effective Hamiltonian of decay $B_c \rightarrow D_s^* \ell^+ \ell^-$

We calculate exclusive semileptonic B meson decay  $B_c \rightarrow D_s^* \ell^+ \ell^-$  with in SM and beyond. The decay corresponds to penguin diagram which is also called SD diagram as shown in Fig.4.1.

The Amplitude for  $B_c \rightarrow D_s^* \ell^+ \ell^-$  which is based on quark level transition of  $b \rightarrow s \ell^+ \ell^-$  decay leaded by effective Hamiltonian from eq.3.9 written as follow;

$$\begin{aligned}
 \mathcal{M}_{B_c \rightarrow D_s^* \bar{\ell} \ell}^{PEGN} = & - \frac{G_F \alpha}{\sqrt{2} \pi} V_{tb} V_{ts}^* [\mathcal{C}_9^{tot}(\mu) \langle D_s^*(k, \epsilon) | \bar{s} \gamma_\mu (1 - \gamma_5) b | B_c(p) \rangle (\bar{\ell} \gamma^\mu l) \\
 & + \mathcal{C}_{10}^{tot} \langle D_s^*(k, \epsilon) | (\bar{s} \gamma_\mu (1 - \gamma_5) b) | B_c(p) \rangle (\bar{\ell} \gamma^\mu \gamma^5 l) \\
 & - 2 \mathcal{C}_7^{eff}(\mu) \frac{m_b}{q^2} \langle D_s^*(k, \epsilon) | (\bar{s} i \sigma_{\mu\nu} q^\nu (1 + \gamma_5) b) | B_c(p) \rangle \bar{\ell} \gamma^\mu l] \quad (4.1)
 \end{aligned}$$

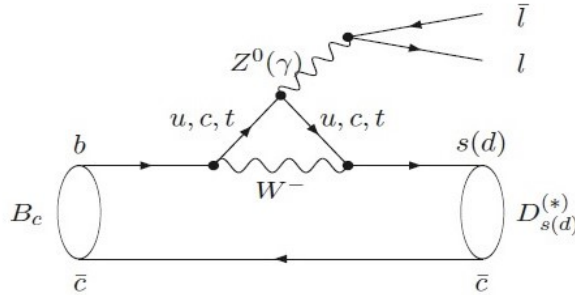


Figure 4.1: Penguin diagram for  $B_c \rightarrow D_s^* \ell^+ \ell^-$  decay [3]



Here,  $C_9^{tot} = C_9^{eff}(\text{SM}) + C_9^{\mu\mu}(\text{NP})$  and  $C_{10}^{tot} = C_{10}^{eff}(\text{SM}) + C_{10}^{\mu\mu}(\text{NP})$ . We write wilson coefficient  $C_9^{eff}$  [17] as

$$C_9^{eff}(\mu) = \mathcal{Y}_{SD}(r, v') + \mathcal{Y}_{LD}(r, v') + C_9(\mu) \quad (4.2)$$

$$C_9^{eff} = C_9 + C_0 \{u(r, v') + \frac{3\pi}{\alpha^2} \Delta \sum_{D_i=\Psi(1s), \Psi(2s)} \frac{\Gamma(D_i \rightarrow l^+l^-) m_{D_i}}{m^2 D_i} - q^2 - im_{D_i} \Gamma D_i\} \quad (4.3)$$

So here,

$$C_0 \equiv 3C_5 + C_6 + 3C_1 + C_2 + 3C_3 + C_4$$

$$\begin{aligned} \mathcal{Y}_{SD}(r, v') &= u(r, v')(3C_1(\mu) + C_2(\mu) + 3C_3(\mu) + C_4(\mu) + 3C_5(\mu) + C_6(\mu)) \\ &\quad - \frac{1}{2}u(1, v')(4C_3(\mu) + 4C_4(\mu) + 3C_5(\mu) + C_6(\mu)) \\ &\quad - \frac{1}{2}u(0, v')(C_3(\mu) + 3C_4(\mu)) + \frac{2}{9}(3C_3(\mu) \\ &\quad + C_4(\mu) + 3C_5(\mu) + C_6(\mu)). \end{aligned}$$

$$\begin{aligned} u(r, v') &= -\frac{8}{9} \ln \frac{m_b}{\mu} - \frac{8}{9} \ln r + \frac{8}{27} + \frac{4}{9}y \\ &\quad - \frac{2}{9}|1-y|^{1/2}(2+y) \left[ \ln \left| \frac{\sqrt{1-y}+1}{\sqrt{1-y}-1} \right| - i\pi \right] \quad \text{for } y \equiv 4r^2/v' < 1, \end{aligned}$$

$$\begin{aligned} u(r, v') &= -\frac{8}{9} \ln \frac{m_b}{\mu} - \frac{8}{9} \ln r + \frac{8}{27} + \frac{4}{9}y \\ &\quad - \frac{2}{9}|1-y|^{1/2}(2+y) \left[ 2 \arctan \frac{1}{\sqrt{y-1}} \right] \quad \text{for } y \equiv 4r^2/v' > 1, \end{aligned}$$

$$u(0, v') = \frac{8}{27} - \frac{8}{9} \ln \frac{m_b}{\mu} - \frac{4}{9} \ln v + \frac{4}{9}i\pi.$$

where  $r = m_c/m_B$ ,  $v' = q^2/m_B^2$  and  $\Delta = 1/C_0$ .  $\mathcal{Y}_{SD}$  denotes the SD contributions.

## 4.2 Matrix Element and Form Factors

The parameterization of matrix elements for decay  $B_c \rightarrow D_s^*$  are written in terms of form factors [2] which are functions of momentum transfer [ $q^2 = (p - k)^2$ ].

$$\begin{aligned}
\langle D_s^*(k, \epsilon) | \bar{s} \gamma_\mu b | B_c(p) \rangle &= \frac{2i \epsilon_{\mu\nu\alpha\beta}}{M_{B_c} + M_{D_s^*}} \epsilon^{*\nu} p^\alpha k^\beta A_V(q^2) \\
\langle D_s^*(k, \epsilon) | \bar{s} \gamma_\mu \gamma_5 b | B_c(p) \rangle &= (M_{B_c} + M_{D_s^*}) \epsilon^{*\mu} A_0(q^2) \\
&\quad - \frac{(\epsilon^* \cdot q) A_+(q^2)}{M_{B_c} + M_{D_s^*}} (p + k)^\mu \\
&\quad - \frac{A_-(q^2)}{M_{B_c} + M_{D_s^*}} (\epsilon^* \cdot q) q^\mu \\
\langle D_s^*(k, \epsilon) | \bar{s} i \sigma_{\mu\nu} q^\nu b | B_c(p) \rangle &= 2i \epsilon_{\mu\nu\alpha\beta} \epsilon^{*\nu} p^\alpha k^\beta T_1(q^2) \\
\langle D_s^*(k, \epsilon) | \bar{s} i \sigma_{\mu\nu} q^\nu \gamma_5 b | B_c(p) \rangle &= \left[ (M_{B_c}^2 + M_{D_s^*}^2) \epsilon_\mu^* - (\epsilon^* \cdot q) (p + k)_\mu \right] T_2(q^2) \\
&\quad + (\epsilon^* \cdot q) \left[ q_\mu - \frac{q^2}{(M_{B_c}^2 + M_{D_s^*}^2)} (p + k)_\mu \right] T_3(q^2)
\end{aligned} \tag{4.4}$$

where  $p$  denotes the momentum of  $B_c$  meson and  $\epsilon(k)$  are the polarization vector  $D_s^*$  meson.

The form factors [2]  $A_V(q^2)$ ,  $A_0(q^2)$ ,  $A_+(q^2)$ ,  $A_-(q^2)$ ,  $T_1(q^2)$ ,  $T_2(q^2)$ ,  $T_3(q^2)$  are the non-perturbative quantities. Form factors are calculated by using QCD sum rules [2]. We use the parameterization of form factors which depends on momentum transfer ( $q^2$ ) can be written as; [2]

$$\mathcal{F}(q^2) = \frac{\mathcal{F}(0)}{1 + \alpha \frac{q^2}{M_{B_c}^2} + \beta \frac{q^4}{M_{B_c}^4}} \tag{4.5}$$

where the values of  $\mathcal{F}(0)$ ,  $\alpha$  and  $\beta$  are given in following Table 4.1.

In order to analyze the various observables, such as the branching ratios, the longitudinal helicity fractions, leptons forward backward asymmetry and lepton flavor Universality(LFU) ratios, we can express the amplitude in helicity basis.

## 4.3 Helicity Amplitude of B meson decay

We write the amplitude of penguin diagram by substituting matrix elements in eq.4.1 and separated out leptonic vector current and leptonic axial current.

| $\mathcal{F}(q^2)$ | $\mathcal{F}(0)$ | $\alpha$ | $\beta$ |
|--------------------|------------------|----------|---------|
| $A_V(q^2)$         | 0.54             | -1.28    | -0.23   |
| $A_0(q^2)$         | 0.30             | -0.13    | -0.18   |
| $A_+(q^2)$         | 0.36             | -0.67    | -0.066  |
| $A_-(q^2)$         | -0.57            | -1.11    | -0.14   |
| $T_1(q^2)$         | 0.31             | -1.28    | -0.23   |
| $T_2(q^2)$         | 0.33             | -0.10    | -0.097  |
| $T_3(q^2)$         | 0.29             | -0.91    | 0.007   |

Table 4.1: Form factors of  $B_c \rightarrow D_s^*$  decay which are calculated by using QCD Sum rules [2].

$$\mathcal{M}_{B_c \rightarrow D_s^* \ell^+ \ell^-}^{PEGN} = -\frac{G_F \alpha}{2\sqrt{2}\pi} V_{tb} V_{ts}^* [T_\mu^1(\bar{l}\gamma^\mu l) + T_\mu^2(\bar{l}\gamma^\mu \gamma^5 l)] \quad (4.6)$$

$$\begin{aligned} T_\mu^1 &= -i\epsilon_{\mu\nu\alpha\beta} \varepsilon^{*\nu} p^\alpha k^\beta \mathcal{F}_1(q^2) - g_{\mu\nu} \mathcal{F}_2(q^2) + q_\mu q_\nu \mathcal{F}_3(q^2) + P_\mu q_\nu \mathcal{F}_4(q^2) \\ T_\mu^2 &= -i\epsilon_{\mu\nu\alpha\beta} \varepsilon^{*\nu} p^\alpha k^\beta \mathcal{F}_5(q^2) - g_{\mu\nu} \mathcal{F}_6(q^2) + q_\mu q_\nu \mathcal{F}_7(q^2) + P_\mu q_\nu \mathcal{F}_8(q^2) \end{aligned}$$

The functions  $\mathcal{F}_1$  to  $\mathcal{F}_8$  in eq. 4.7 are recognized as auxiliary functions. Auxiliary functions contain both SD (WC's) and LD (Form factors).

We write the auxiliary functions as follow;

$$\begin{aligned} \mathcal{F}_1 &= \frac{2C_9^{eff} A_V(q^2)}{M_{D_s^*} + M_{B_c}} + \frac{4m_b}{q^2} C_7^{eff} T_1(q^2) \\ \mathcal{F}_2 &= C_9^{eff} A_0(q^2)(M_{D_s^*} + M_{B_c}) + \frac{2m_b}{q^2} C_7^{eff} T_2(q^2)(M_{D_s^*} + M_{B_c}) \\ \mathcal{F}_3 &= \frac{A_-(q^2) C_9^{eff}}{M_{D_s^*} + M_{B_c}} + \frac{2m_b}{q^2} C_7^{eff} T_3(q^2) \\ \mathcal{F}_4 &= \frac{A_+(q^2) C_9^{eff}}{M_{D_s^*} + M_{B_c}} + \frac{2m_b}{q^2} (T_2(q^2) + \frac{q^2 T_3(q^2)}{M_{D_s^*} + M_{B_c}}) \\ \mathcal{F}_5 &= \frac{2C_{10}^{eff} A_V(q^2)}{M_{D_s^*} + M_{B_c}} \\ \mathcal{F}_6 &= C_{10}^{eff} (M_{D_s^*} + M_{B_c}) A_0(q^2) \\ \mathcal{F}_7 &= \frac{C_{10}^{eff} A_-(q^2)}{M_{D_s^*} + M_{B_c}} \\ \mathcal{F}_8 &= \frac{C_{10}^{eff} A_+(q^2)}{M_{D_s^*} + M_{B_c}} \end{aligned} \quad (4.7)$$

Now square of amplitude modulus is written as;

$$|M|^2 = M^\dagger M$$

$$|M|^2 = \frac{G_f \alpha \lambda_t}{2\sqrt{2}\pi} [T_1^\mu T_1^{\dagger\nu} (\bar{l}\gamma_\mu l)(\bar{l}\gamma_\nu l)^\dagger + T_1^\mu T_2^{\dagger\nu} (\bar{l}\gamma_\mu l)(\bar{l}\gamma_\nu \gamma_5 l)^\dagger + T_2^\mu T_1^{\dagger\nu} (\bar{l}\gamma_\nu \gamma_5 l)(\bar{l}\gamma_\mu l)^\dagger + T_2^\mu T_2^{\dagger\nu} (\bar{l}\gamma_\mu \gamma_5 l)(\bar{l}\gamma_\nu \gamma_5 l)^\dagger] \quad (4.8)$$

$$|M|^2 = \frac{G_f \alpha \lambda_t}{2\sqrt{2}\pi} [H_{11}^{\mu\mu} (\bar{l}\gamma_\mu l)(\bar{l}\gamma_\nu l)^\dagger + H_{12}^{\mu\nu} (\bar{l}\gamma_\mu l)(\bar{l}\gamma_\nu \gamma_5 l)^\dagger + H_{21}^{\mu\nu} (\bar{l}\gamma_\nu \gamma_5 l)(\bar{l}\gamma_\mu l)^\dagger + H_{22}^{\mu\mu} (\bar{l}\gamma_\mu \gamma_5 l)(\bar{l}\gamma_\nu \gamma_5 l)^\dagger] \quad (4.9)$$

Where  $\lambda_t = V_{tb} V_{ts}^*$  and  $H_{ij}^{\mu\nu} = T_i^\mu T_j^{\nu\dagger}$

now as,

$$(\bar{l}\gamma_\mu l)(\bar{l}\gamma_\nu l)^\dagger = \text{tr}[\gamma^\mu (p_1^\mu - m_l) \gamma_\nu (p_2^\mu + m_l)] \quad (4.10)$$

$$(\bar{l}\gamma_\mu l)(\bar{l}\gamma_\nu \gamma_5 l)^\dagger = \text{tr}[\gamma^\mu \gamma_5 (p_1^\mu - m_l) \gamma_\nu \gamma_5 (p_2^\mu + m_l)]$$

$$(\bar{l}\gamma_\nu \gamma_5 l)(\bar{l}\gamma_\mu l)^\dagger = -\text{tr}[\gamma^\mu (p_1^\mu - m_l) \gamma_\nu \gamma_5 (p_2^\mu + m_l)]$$

$$(\bar{l}\gamma_\mu \gamma_5 l)(\bar{l}\gamma_\nu \gamma_5 l)^\dagger = -\text{tr}[\gamma^\mu \gamma_5 (p_1^\mu - m_l) \gamma_\nu (p_2^\mu + m_l)]$$

so therefore,

$$\sum_{pol} |M|^2 = [H_{11}^{\mu\mu} \cdot \text{tr}[\gamma^\mu (p_1^\mu - m_l) \gamma_\nu (p_2^\mu + m_l)] + H_{22}^{\mu\nu} \cdot \text{tr}[\gamma^\mu \gamma_5 (p_1^\mu - m_l) \gamma_\nu \gamma_5 (p_2^\mu + m_l)] - H_{12}^{\mu\nu} \cdot \text{tr}[\gamma^\mu (p_1^\mu - m_l) \gamma_\nu \gamma_5 (p_2^\mu + m_l)] - H_{21}^{\mu\nu} \cdot \text{tr}[\gamma^\mu \gamma_5 (p_1^\mu - m_l) \gamma_\nu (p_2^\mu + m_l)]] \quad (4.11)$$

$$= [H_{11}^{\mu\nu} \cdot A(-g_{\mu\nu}(m_l^2 + p_1 \cdot p_1) + p_1^\mu p_2^\nu + p_2^\mu p_1^\nu) + H_{22}^{\mu\nu} \cdot A(g_{\mu\nu}(m_l^2 - p_1 \cdot p_1) + p_1^\mu p_2^\nu + p_2^\mu p_1^\nu) + H_{12}^{\mu\nu} \cdot A(i\epsilon_{\mu\nu\alpha\beta} p_1^\alpha p_2^\beta) + H_{21}^{\mu\nu} \cdot A(i\epsilon_{\mu\nu\alpha\beta} p_1^\alpha p_2^\beta)] \quad (4.12)$$

$$\begin{aligned}
\sum_{pol} |M|^2 &= 4[H_{11}^{\mu\nu}(-L_{\mu\nu}^{(2)}(m_l^2 + \frac{q^2 - 2m_l^2}{2}) + L_{\mu\nu}^{(1)}) \\
&+ H_{22}^{\mu\nu}(L_{\mu\nu}^{(2)}(m_l^2 + \frac{q^2 - 2m_l^2}{2}) + L_{\mu\nu}^{(1)}) \\
&+ (H_{12}^{\mu\nu} + H_{21}^{\mu\nu})L_{\mu\nu}^{(3)}]
\end{aligned} \tag{4.13}$$

$$\begin{aligned}
\sum_{pol} |M|^2 &= 4[L_{\mu\nu}^{(1)}(H_{11}^{\mu\nu} + H_{22}^{\mu\nu}) - \frac{1}{2}L_{\mu\nu}^{(2)}(q^2 H_{11}^{\mu\nu} + (q^2 - m_l^2)H_{22}^{\mu\nu}) \\
&+ L_{\mu\nu}^{(3)}(H_{12}^{\mu\nu} + H_{21}^{\mu\nu})]
\end{aligned} \tag{4.14}$$

We have defined hadron and lepton tensors [17] as

$$\begin{aligned}
L_{\mu\nu}^{(1)} &= p_{1\mu}p_{2\nu} + p_{2\mu}p_{1\nu} \\
L_{\mu\nu}^{(2)} &= g_{\mu\nu} \\
L_{\mu\nu}^{(3)} &= i\epsilon_{\mu\nu\alpha\beta}p_1^\alpha p_2^\beta \\
H_{ij}^{\mu\nu} &= T_i^\mu T_j^{\nu\dagger}
\end{aligned} \tag{4.15}$$

We will solve these tensors in the following sections.

### 4.3.1 Hadronic part

The hadronic tensor in terms of helicity basis  $\varepsilon^{\dagger\mu}(m)$  as,

$$\begin{aligned}
H_m^i &= \varepsilon^{\dagger\mu}(m)T_\mu^{(i)} \\
H_m^i &= \varepsilon^{\dagger\mu}(m)\varepsilon^{\dagger\nu}(n)T_{\mu\nu}^{(i)}
\end{aligned} \tag{4.16}$$

Where  $T_\mu^{(i)} = \varepsilon^{\dagger\nu}(n)T_{\mu\nu}^{(i)}$ ,  $\varepsilon^\nu$  is the "vector polarization" of the final state  $D_s^*$  meson;  $m, n = 0, \pm, t$ , are the longitudinal, transverse and time components; and  $i = 1, 2$ ; The helicity components of polarization vector reads as;

$$\begin{aligned}
\epsilon^\mu(\pm) &= \frac{1}{\sqrt{2}}(0, \pm 1, i, 0) \\
\epsilon^\mu(0) &= \frac{1}{m}(|k|, 0, 0, E) \\
g_{mn} &= \text{diag}(+, -, -, -)
\end{aligned} \tag{4.17}$$

and in the  $B$ -meson rest frame i.e

$$\begin{aligned}
p^\mu &= (m_B, 0, 0, 0) \\
k^\mu &= (E_k, 0, 0, |k|) \\
q^\mu &= (q_0, 0, 0, |k|)
\end{aligned} \tag{4.18}$$

the polarization vectors reads as

$$\begin{aligned}
\varepsilon^\mu(t) &= \frac{1}{\sqrt{q^2}}(q_0, 0, 0, |k|) \\
\varepsilon^\mu(\pm) &= \frac{1}{\sqrt{2}}(0, \mp 1, i, |k|) \\
\varepsilon^\mu(0) &= \frac{1}{\sqrt{q^2}}(|k|, 0, 0, q_0)
\end{aligned} \tag{4.19}$$

where  $|k| = \frac{\sqrt{\lambda}}{2m_B}$ ;  $\lambda = m_B^4 + m_{D_s^*}^4 + q^4 - 2(m_B^2 m_{D_s^*}^2 + m_{D_s^*}^2 q^2 + m_B^2 q^2)$  and  $E_{D_s^*} = \frac{m_B^2 + m_{D_s^*}^2 - q^2}{2m_B}$ ,  $D_s^*$  is final state meson, so using equation of Hadronic tensor we have,

$$\begin{aligned}
H_0^{(1)} &= \frac{1}{m_{D_s^*} \sqrt{q^2}} [2q_0 |k|^2 (q_0 - E_{D_s^*}) \mathcal{F}_2 + (|k|^2 + q_0 E_{D_s^*}) \mathcal{F}_3 \\
&\quad + |k|^2 (q_0 (m_B + 2E_{D_s^*}) - q_0^2 - E_{D_s^*} (m_B + E_{D_s^*})) \mathcal{F}_4] \\
H_0^{(2)} &= \frac{1}{m_{D_s^*} \sqrt{q^2}} [2q_0 |k|^2 (q_0 - E_{D_s^*}) \mathcal{F}_6 + (|k|^2 + q_0 E_{D_s^*}) \mathcal{F}_7 \\
&\quad + |k|^2 (q_0 (m_B + 2E_{D_s^*}) - q_0^2 - E_{D_s^*} (m_B + E_{D_s^*})) \mathcal{F}_8] \\
H_+^{(1)} &= -i|k| m_B \mathcal{F}_1 + \mathcal{F}_3 \\
H_+^{(2)} &= -i|k| m_B \mathcal{F}_5 + \mathcal{F}_7 \\
H_-^{(1)} &= i|k| m_B \mathcal{F}_1 + \mathcal{F}_3 \\
H_-^{(2)} &= i|k| m_B \mathcal{F}_5 + \mathcal{F}_7
\end{aligned} \tag{4.20}$$

These are the components of hadronic tensor, The subscripts  $\pm, 0$  denotes the transverse and longitudinal helicity components, respectively. We have ignored the time component for both leptonic and hadronic tensors.

### 4.3.2 Leptonic Part

For the leptonic tensors  $L_{\mu\nu}^{(k)}$  in  $\bar{l}l$ -CM frame we can write,

$$\begin{aligned}
q^\mu &= (\sqrt{q^2}, \vec{0}) \\
p_1^\mu &= (E_l, |p_1| \sin\theta, 0, |p_1| \cos\theta) \\
p_2^\mu &= (E_l, -|p_1| \sin\theta, 0, -|p_1| \cos\theta)
\end{aligned} \tag{4.21}$$

with  $E_l = \sqrt{q^2}/2$  and  $|p_1| = \sqrt{q^2 - 4m_l^2}/2$  and the polarization vectors in  $\bar{l}l - CM$  frame are;

$$\begin{aligned}\epsilon^\mu(\pm) &= \frac{1}{\sqrt{2}}(0, \pm 1, i, 0) \\ \epsilon^\mu(0) &= (0, 0, 0, 1) \\ \epsilon^\mu(t) &= (1, 0, 0, 0)\end{aligned}\tag{4.22}$$

Hence by using this information of polarization of vectors and lepton kinematics, we have calculated the following lepton tensor components;

$$\begin{aligned}L_{00}^1 &= -2|p_1|^2 \cos^2\theta \\ L_{00}^2 &= -1 \\ L_{00}^3 &= 0 \\ L_{++}^1 &= E_l - |p_1|^2 \sin^2\theta \\ L_{++}^2 &= -1 \\ L_{++}^3 &= -2E_l|p_1| \cos\theta \\ L_{--}^1 &= E_l^2 \\ L_{--}^2 &= -1 \\ L_{--}^3 &= 2E_l|p_1| \cos\theta\end{aligned}\tag{4.23}$$

Now, by using these leptonic tensor components, the hadronic tensor components, we can write amplitude  $\mathcal{M}$  of saai decay in terms of helicity basis.

## 4.4 Differential decay rate

We write branching ratio in terms of helicity amplitude, which is:

$$\begin{aligned}\frac{d^2\Gamma(B_c \rightarrow D_s^* \ell^+ \ell^-)}{dq^2} &= \frac{1}{(2\pi)^3} \frac{1}{32M_{B_c}^3} \int_{+(q^2)}^{-(q^2)} dq^2 |\mathcal{M}|^2 \\ \frac{d^2\Gamma(B_c \rightarrow D_s^* \ell^+ \ell^-)}{dq^2 d\cos\theta} &= \frac{G_F^2}{(2\pi)^3} \left( \frac{\alpha|\lambda_t|}{2\pi} \right)^2 \frac{|k|\sqrt{1-4m_l^2/q^2}}{8m_l^2} \frac{1}{2} [ L_{\mu\nu}^{(1)} \cdot (H_{11}^{\mu\nu} + H_{22}^{\mu\nu}) \\ &\quad - \frac{1}{2} L_{\mu\nu}^{(2)} (q^2 H_{11}^{\mu\nu} + (q^2 - m_l^2) H_{22}^{\mu\nu}) + L_{\mu\nu}^{(3)} \cdot (H_{12}^{\mu\nu} + H_{21}^{\mu\nu}) ]\end{aligned}\tag{4.24}$$

Where  $\lambda_t = |V_{ts}^\dagger V_{tb}|$  denotes CKM matrices,  $|k|$  denotes as momentum of vector meson given in the rest frame of  $B$  meson. After integration over  $\cos\theta$  and putting the values of the leptonic and hadronic tensor components  $L^{(k)}(m, n)$ ,  $H^{ij}(m, n)$  respectively, we get;

$$\frac{d\Gamma(B \rightarrow D_s^* \ell^+ \ell^-)}{dq^2} = \frac{G_F^2}{(2\pi)^3} \left( \frac{\alpha |\lambda_t|}{2\pi} \right)^2 \frac{\lambda^{1/2} q^2}{48M_B^3} \sqrt{1 - 4m_\ell^2/q^2} [ H^1 H^{1\dagger} (1 + 4m_\ell^2/q^2) + H^2 H^{2\dagger} (1 - 4m_\ell^2/q^2) ] \quad (4.26)$$

where  $m_\ell$  denotes as the lepton mass,  $\lambda = M_B^4 + M_{D_s^*}^4 + q^4 - 2(M_B^2 M_{D_s^*}^2 + M_{D_s^*}^2 q^2 + M_B^2 q^2)$  and we separated out transverse and longitudinal hadronic components of amplitudes.

$$H^i H^{i\dagger} \equiv H_+^i H_+^{i\dagger} + H_-^i H_-^{i\dagger} + H_0^i H_0^{i\dagger}$$

Branching ratios precisely used in literature to find NP effects. NP effects can be observe more easily in the branching ratio of  $B_c \rightarrow D_s^* \ell^+ \ell^-$  than others observables because branching ratios are measured to be consistent with both the SM and NP.

## 4.5 Forward Backward Asymmetry

We determine leptons forward backward asymmetry(FBA) to analyze our said process. FBA is an importance observables to search NP effects than the other physical observables because its minimize the uncertainties due to form factors and the value of zero crossing of  $\mathcal{A}_{FB}$  gives a more clear signal of presence of NP effects.

The FBA of leptons is defined as;

$$\mathcal{A}_{FB} = \frac{\mathcal{N}^F - \mathcal{N}^B}{\mathcal{N}^F + \mathcal{N}^B} \quad (4.27)$$

where  $\mathcal{N}^F(\mathcal{N}^B)$  is the number of event in which leptons moving in forward(backward) directions.

We use the double differential decay rate formula from eq. 4.26 to simplify the following expression for forward backward asymmetries;

$$\mathcal{A}_{FB}(q^2) = \frac{\int_0^1 d\cos\theta \frac{d^2\Gamma(q^2, \cos\theta)}{dq^2 d\cos\theta} - \int_{-1}^0 d\cos\theta \frac{d^2\Gamma(q^2, \cos\theta)}{dq^2 d\cos\theta}}{\int_0^1 d\cos\theta \frac{d^2\Gamma(q^2, \cos\theta)}{dq^2 d\cos\theta} + \int_{-1}^0 d\cos\theta \frac{d^2\Gamma(q^2, \cos\theta)}{dq^2 d\cos\theta}} \quad (4.28)$$

We write the analytical expression for forward backward Asymmetry of leptons as follow;

$$\mathcal{A}_{FB} = \frac{3}{4} \sqrt{1 - \frac{4m_\ell^2}{q^2}} \frac{Re(H_+^{(1)} H_+^{\dagger(2)}) - Re(H_-^{(1)} H_-^{\dagger(2)})}{H^{(1)} H^{\dagger(1)} (1 + \frac{4m_\ell^2}{q^2}) + H^{(2)} H^{\dagger(2)} (1 - \frac{4m_\ell^2}{q^2})} \quad (4.29)$$



## 4.6 Helicity Fraction

Longitudinal Helicity fraction of  $D_s^*$  meson in said decay which have less dependence on input parameters and uncertainties arising because of form factors. The study of helicity fraction will give a test for NP in said process.

We write an differential expression for longitudinal helicity fraction of  $D_s^*$  meson;

$$F_L = \frac{d\Gamma_L(q^2)/dq^2}{d\Gamma(q^2)/dq^2} \quad (4.30)$$

where  $d\Gamma_L(q^2)/dq^2$  is the longitudinal component of decay rate. Now we can easily write the following analytical expression for longitudinal helicity fraction by using longitudinal and total component of decay rate in eq.4.30;

$$F_L(q^2) = \frac{H_0^{(1)} H_0^{(1)\dagger} (1 + \frac{4m_l^2}{q^2}) + H_0^{(2)} H_0^{(2)\dagger} (1 - \frac{4m_l^2}{q^2})}{H^{(1)} H^{(1)\dagger} (1 + \frac{4m_l^2}{q^2}) + H^{(2)} H^{(2)\dagger} (1 - \frac{4m_l^2}{q^2})} \quad (4.31)$$

The experimentally measured values of  $F_L^{K^*}$  for the decay  $B \rightarrow K^* \ell^+ \ell^-$  based on transition of  $b \rightarrow s \bar{\ell}^+ \ell^-$  by Babar collaboration are [31]

$$F_L^{[q^2 \leq 10.24]} = 0.51_{-0.25}^{+0.22} \pm 0.08 \quad (4.32)$$

$$F_L^{[0.1, 8.14]} = 0.77_{-0.30}^{+0.63} \pm 0.07 \quad (4.33)$$

these values have tension with SM prediction. Longitudinal helicity fraction of  $D_s^*$  meson may hint the influence of NP in said decay.

## 4.7 Lepton Flavor Universality Ratios

Lepton Flavor Universality ratios are the ratio of branching ratios to different lepton generation and this observable an ideal tool to test for NP in said process. We compare cross sections or decay widths which change only in lepton flavor, like electron and muon, So lepton flavor universality ratios can be represented as a function of particle masses where CKM matrix element factors and guage factor void in ratios, although hadronic physics parameters like as form factors and decay constants also suppress in LFU ratios.

Analytical expression for LFU ratio can be written as;

$$R_{D_s^{(*)}} = \frac{\int_{q_{min}^2}^{q_{max}^2} \frac{d\mathcal{B}(B_c \rightarrow D_s^{(*)} \mu^+ \mu^-)}{dq^2} dq^2}{\int_{q_{min}^2}^{q_{max}^2} \frac{d\mathcal{B}(B_c \rightarrow D_s^{(*)} e^+ e^-)}{dq^2} dq^2} \quad (4.34)$$

Deviation in LFU ratio from the SM predictions is the good sign of the presence of NP. So experimentally measured LFU ratios at LHCb are theoretically very clean observable in the

search of NP and the values given by LHCb are [32, 33]

$$R_{K^*}^{[1,1,6]} = 0.69_{-0.07}^{+0.11} \pm 0.05, R_K^{[1,6]} = 0.745_{-0.074}^{+0.090} \pm 0.036, R_{K^*}^{[0.045,1.1]} = 0.66_{-0.07}^{+0.01} \pm 0.03 \quad (4.35)$$

these values have deviation with the SM values are  $2.1\text{-}2.3\sigma$ ,  $2.6\sigma$  and  $2.6\sigma$  respectively [34]. The measurements of the ratios  $R_{K^*}$  hint towards LFU violation. We test lepton flavor universality ratio in rare  $B$  meson decays where interestingly large hadronic uncertainties essentially cancel out. We will consider MI new physics scenarios and  $Z'$  models to deduce NP effects by LFU ratios, so we will determine to which pattern new physics effects arises in  $R_{D_s^*}$ .

| Observables   | [0.045-1] | [1-2]  | [2-3]  | [3-4] | [4-5] | [5-6] | [1-6] |
|---|-----------|--------|--------|-------|-------|-------|-------|
| $10^{-7} \times \mathcal{B}(B_c \rightarrow D_s^* \mu^+ \mu^-)$ | 0.213     | 0.071  | 0.078  | 0.094 | 0.011 | 0.012 | 0.048 |
| $\langle R_{D_s^*} \rangle$                                     | 0.939     | 0.977  | 0.981  | 0.985 | 0.989 | 0.991 | 0.985 |
| $\langle F_{D_s^*}^L \rangle$                                   | 0.177     | 0.617  | 0.564  | 0.469 | 0.397 | 0.345 | 0.458 |
| $\langle A_{FB} \rangle$  | -0.023    | -0.055 | -0.022 | 0.003 | 0.020 | 0.031 | 0.001 |

Table 4.2: In different  $q^2$  bins: averaged values in different observables of  $B_c \rightarrow D_s^* \mu^+ \mu^-$  decay in the SM.

## 4.8 Phenomenological Analysis

In the numerical calculation, we state all the inputs that are used for our various observables. Renormalization scale is  $\mu = 4.8\text{GeV}$  in our analysis. Mass of fermions, we use  $m_b = 4.18\text{GeV}$ ,  $m_\mu = 0.015\text{GeV}$ ,  $m_c = 1.28\text{GeV}$ . Mass of mesons, we use  $M_{B_c} = 6.23\text{GeV}$ ,  $M_{D_s^*} = 2.112\text{GeV}$ . Similarly,  $B_c$  meson mean life time is  $\tau_{B_c} = 0.507 \times 10^{-12}$  and  $G_F = 1.15 \times 10^{-5}\text{GeV}^{-2}$  is fermi coupling constant which are given in ref. [2]. We take  $\alpha_e^{-1} = 137$  for the electromagnetic coupling constant. We use CKM matrix element  $|V_{tb}V_{ts}^*| = 38.5 \times 10^{-3}$  [2]. The WC's are taken from ref. [2] given in table 4.3. For MI scenarios, we use the wilson coefficient given in table 3.1. We take wilson coefficients of model independent scenario II to deduce new physics effects in LQ model. For  $Z'$  models, we use wilson coefficients couplings given in tables 3.2, 3.3, 3.4.

| $\mathcal{C}_1$ | $\mathcal{C}_2$ | $\mathcal{C}_3$ | $\mathcal{C}_4$ | $\mathcal{C}_5$ | $\mathcal{C}_6$ | $\mathcal{C}_7^{eff}$ | $\mathcal{C}_8$ | $\mathcal{C}_9$ | $\mathcal{C}_{10}$ |
|-----------------|-----------------|-----------------|-----------------|-----------------|-----------------|-----------------------|-----------------|-----------------|--------------------|
| -0.2632         | 1.0111          | 0.0055          | -0.0806         | 0.0004          | 0.0009          | -0.313                | -0.15           | 4.0749          | -4.3085            |

Table 4.3: The values of WCs  $\mathcal{C}_i(\mu)$  [2] at the scale  $\mu = 4.8\text{GeV}$  shown in above table.

Like  $B \rightarrow D^{(*)}\tau\nu$  and  $B \rightarrow K^{(*)}\mu^+\mu^-$  decays which are precisely studied [32, 33], the  $B_c \rightarrow D_s^*\mu^+\mu^-$  decay also provide complimentary information regarding NP. From several years, many observables related to the FCNC transitions  $b \rightarrow s\ell^+\ell^-$  have shown deviation from SM expectations. These transitions are well known to have a high sensitivity to NP

contributions due to their suppression within the SM. We show the results achieved in  $Z'$  models and model independent/ leptoquark model which have deviation from corresponding SM predictions.

- We plotted branching ratios of our said decay in model independent new physics scenarios and in model dependent, i.e. leptoquark and  $Z'$  models. In order to search NP effects in mentioned observables discarded the  $\bar{c}c$  resonance region because NP effects are not clear in this region. Branching ratio shows maximum deviation from SM in particular  $q^2$  regions  $4 < q^2 < 6$  and  $6 < q^2 < 8$ . We see in  $4 < q^2 < 6$   $q^2$  region. For MI scenarios I(A), it deviates 21% below the SM. For MI scenarios II(A), it deviates 25% below the SM. For MI scenarios I(B), it deviates 22% below the SM. For MI scenarios II(B), it deviates 28% below the SM. For Heavy  $Z'$  I(A), it deviates 35% above the SM. For Heavy  $Z'$  II(A), it deviates 40% above the SM. For Heavy  $Z'$  I(B), it deviates 37% above the SM. For Heavy  $Z'$  II(B), it deviates 45% above the SM. For light  $Z'$  I(A), it deviates 23% above the SM. For light  $Z'$  II(A), it deviates 34% above the SM, as shown in figs.4.2c4.2d.

We see in  $6 < q^2 < 8$   $q^2$  region. For MI scenarios I(A), it deviates 22% below the SM. For MI scenarios II(A), it deviates 25% below the SM. For MI scenarios I(B), it deviates 23% below the SM. For MI scenarios II(B), it deviates 28% below the SM. For Heavy  $Z'$  I(A), it deviates 35% above the SM. For Heavy  $Z'$  II(A), it deviates 40% above the SM. For Heavy  $Z'$  I(B), it deviates 37% above the SM. For Heavy  $Z'$  II(B), it deviates 44% above the SM. For light  $Z'$  I(A), it deviates 24% above the SM. For light  $Z'$  II(A), it deviates 35% above the SM, as shown in figs.4.2e4.2f. Deviations from SM could also be seen in high  $12 < q^2 < 15$  region as well.

Consequently, we analyze that, for model independent scenarios and leptoquark model, the branching ratio for the decay is decreased at all  $q^2$  from SM as shown in fig.4.2a. For  $Z'$  models, the branching ratio for the decay is increased at all  $q^2$  from the SM as shown in fig.4.2b. Deviations from SM hint the influence of NP in said decay.

- We plotted leptons forward backward asymmetry of our said decay. We analyze that the zero value of forward backward asymmetry  $A_{FB}(q^2)$  is shifted to higher values of  $q^2$  than in the standard model for model independent scenarios and leptoquark model as shown in fig.4.3e. For  $Z'$  model, the zero value of forward backward asymmetry is shifted to lower values of  $q^2$  than in SM which we can see in region  $2.4 < q^2 < 5$  as shown in fig.4.3f. We could not distinguish  $Z'$  models NP scenarios in  $6 < q^2 < 8$   $q^2$  region but we can distinguish in MI new physics scenarios. We see all new physics scenarios separately in the  $1.2 < q^2 < 2.4$  region as shown in figs.4.3c4.3d. We also analyze that model dependent and model independent new physics scenarios didn't show deviation from SM in high  $q^2$  region  $12 < q^2 < 15$  except model independent (I).
- We plotted longitudinal helicity fraction of the  $D_s^*$  meson in model independent scenarios and model dependent for our said decay. Longitudinal helicity fraction have deviation with SM values in low  $0.045 < q^2 < 1.1$   $q^2$  region. For MI scenarios I(A), it deviates 25% below the SM. For MI scenarios II(A), it deviates 29% below the SM. For MI scenarios I(B), it deviates 26% below the SM. For MI scenarios II(B), it deviates

31% below the SM. For Heavy  $Z'$  I(A), it deviates 30% above the SM. For Heavy  $Z'$  II(A), it deviates 28% above the SM. For Heavy  $Z'$  I(B), it deviates 31% above the SM. For Heavy  $Z'$  II(B), it deviates 31% above the SM. For light  $Z'$  I(A), it deviates 14% above the SM. For light  $Z'$  II(A), it deviates 23% above the SM, as shown in figs.4.4a4.4b. Consequently, for model independent scenarios and leptoquark model, the peak of the distribution is decreased at all  $q^2$  and it is on a small scale shifted nearly higher value of  $q^2$  than in the SM as shown in fig.4.4c, and for  $Z'$  Models, the peak of the distribution is increased at all  $q^2$  as shown in fig.4.4d. In longitudinal helicity fraction of  $D_s^*$  meson, we also analyze that all new physics scenarios didn't show deviation from SM in central and high  $q^2$  region.

- We calculated the values of polarized and unpolarized LFU ratios of our said decay in the range of low, central and high  $q^2$  region given in tables4.44.54.6. The calculated values of LFU ratios performed in different  $q^2$  bins have tension with SM predictions. Longitudinally polarized LFU ratios deviates from SM values in low  $0.045 < q^2 < 1$  average bin values that observed from experimental data and SM prediction. For MI scenarios I(A), it deviates 7% below the SM. For MI scenarios II(A), it deviates 2% below the SM. For MI scenarios I(B), it deviates 7% below the SM. For MI scenarios II(B), it deviates 2% below the SM. For Heavy  $Z'$  I(A), it deviates 6% above the SM. For Heavy  $Z'$  II(A), it deviates 7% above the SM. For Heavy  $Z'$  I(B), it deviates 2% above the SM. For Heavy  $Z'$  II(B), it deviates 2% above the SM. For light  $Z'$  I(A), it deviates 4% above the SM. For light  $Z'$  I(A), it deviates 6% above the SM. We observed that for MI and leptoquark model, LFU ratios in low  $q^2$  values are smaller than SM value and for  $Z'$  models, LFU ratios in low  $q^2$  bin values are greater than SM value. In LFU ratios, we analyze that all new physics scenarios didn't show deviation in central and high  $q^2$  region.

#### 4.8.1 Predictions for $R_{D_s^*}, R_{D_s^*}^{L,T}, F_{D_s^*}^L, A_{FB}$ in Different $q^2$ Bins

We give a prediction of  $q^2$  average bin values of several observables in SM and in various NP scenarios such as, the MI scenario/ LQ model and the  $Z'$  models. We predicts these values in different  $q^2$  bins in the following tables.

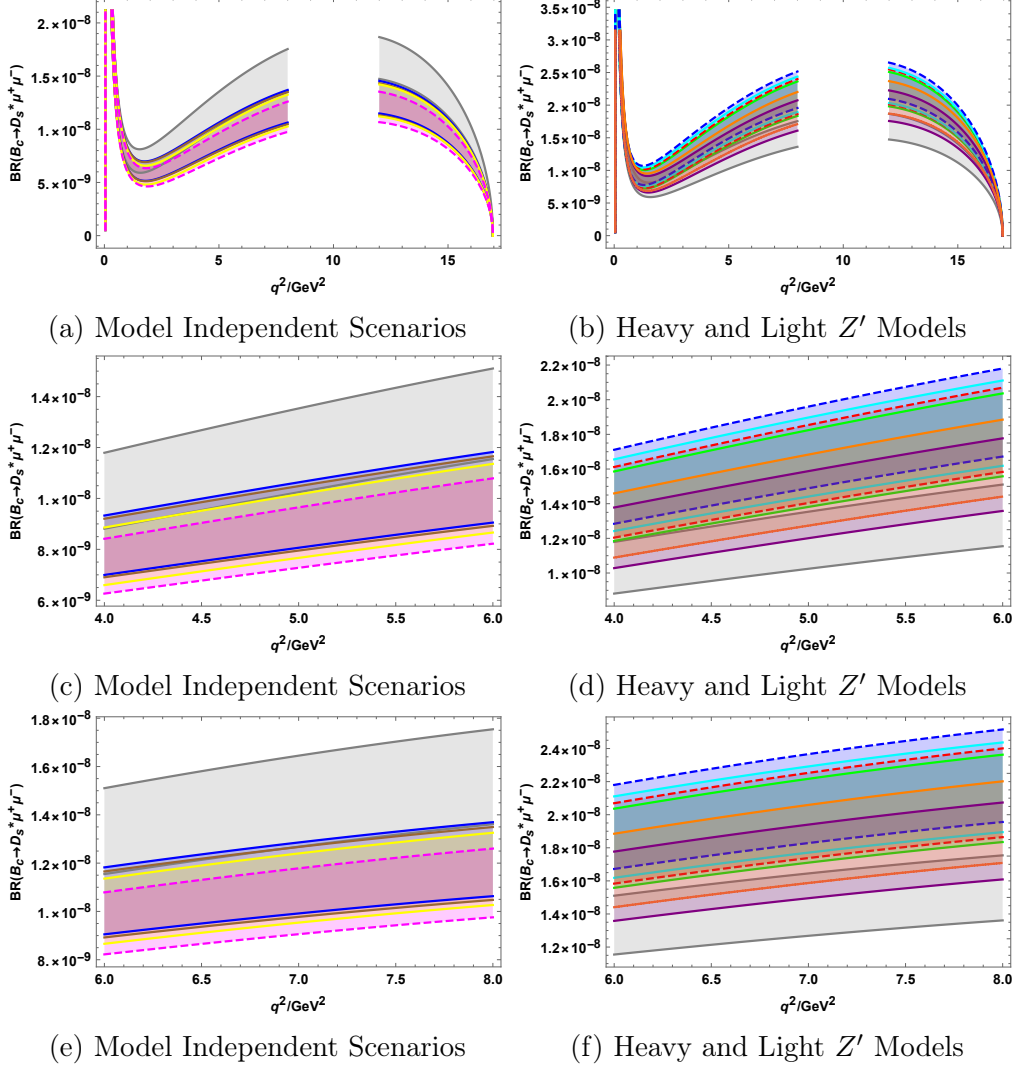


Figure 4.2: Branching ratio in MI Scenarios, Leptoquark Model, Heavy  $Z'$  Model and Light  $Z'$  Model. The Gray band show the predictions in the SM, Blue, Brown, Yellow and Magenta(dashed) bands show the predictions computed in MI scenario I(A), I(B), II(A) and II(B) respectively. Green, Red(dashed), Blue(dashed) and Cyan bands show the predictions computed in scenario  $HZ'$  I(A),  $HZ'$  I(B),  $HZ'$  II(A) and  $HZ'$  II(B) respectively. Purple and Orange bands shows the predictions in scenario  $LZ'$  I(A),  $LZ'$  II(A) respectively. The results achieved in MI scenarios II(A) and II(B) also represent the results in leptoquark model.

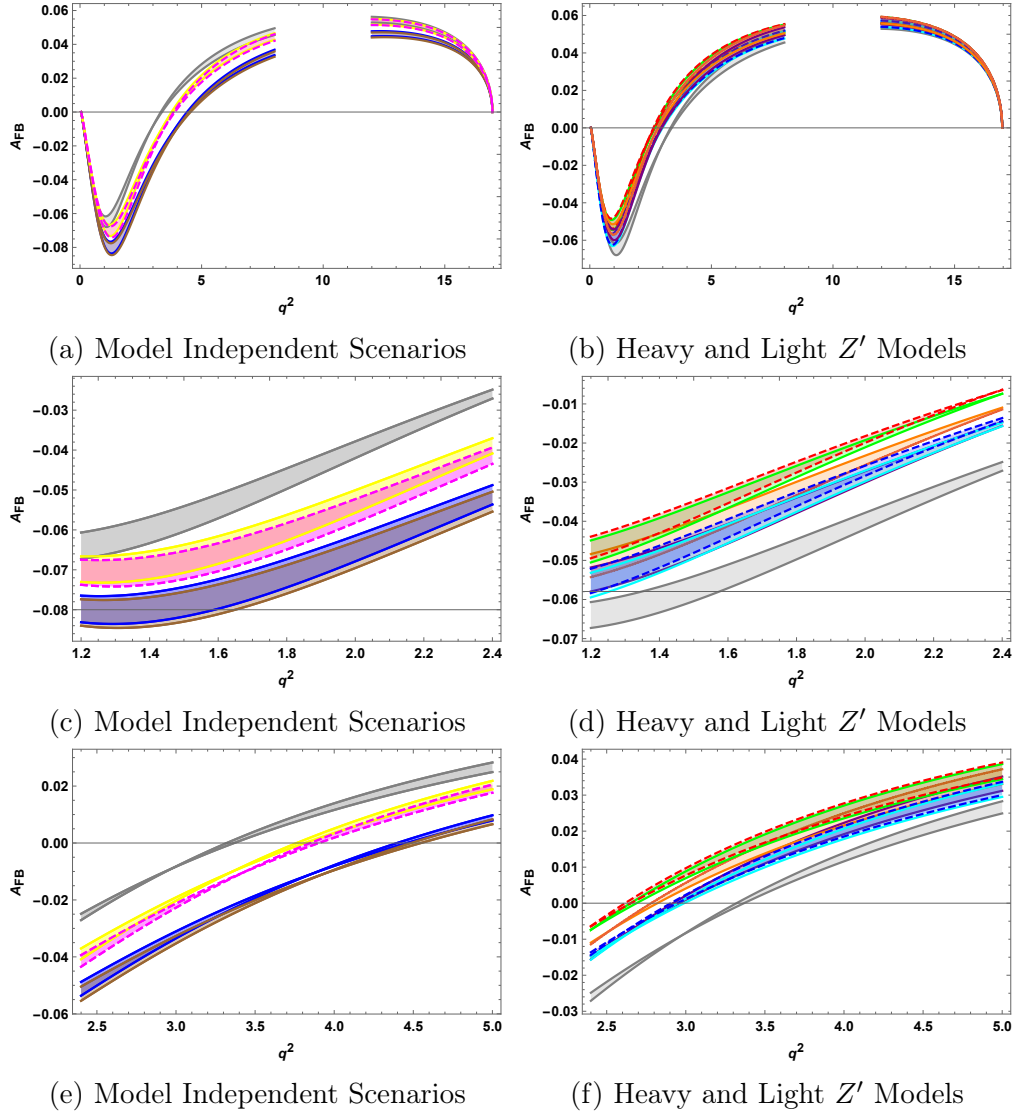


Figure 4.3: Leptons forward backward asymmetry in MI Scenarios, LQ Model, Heavy  $Z'$  Model and Light  $Z'$  Model. The legends are same as in fig.4.2

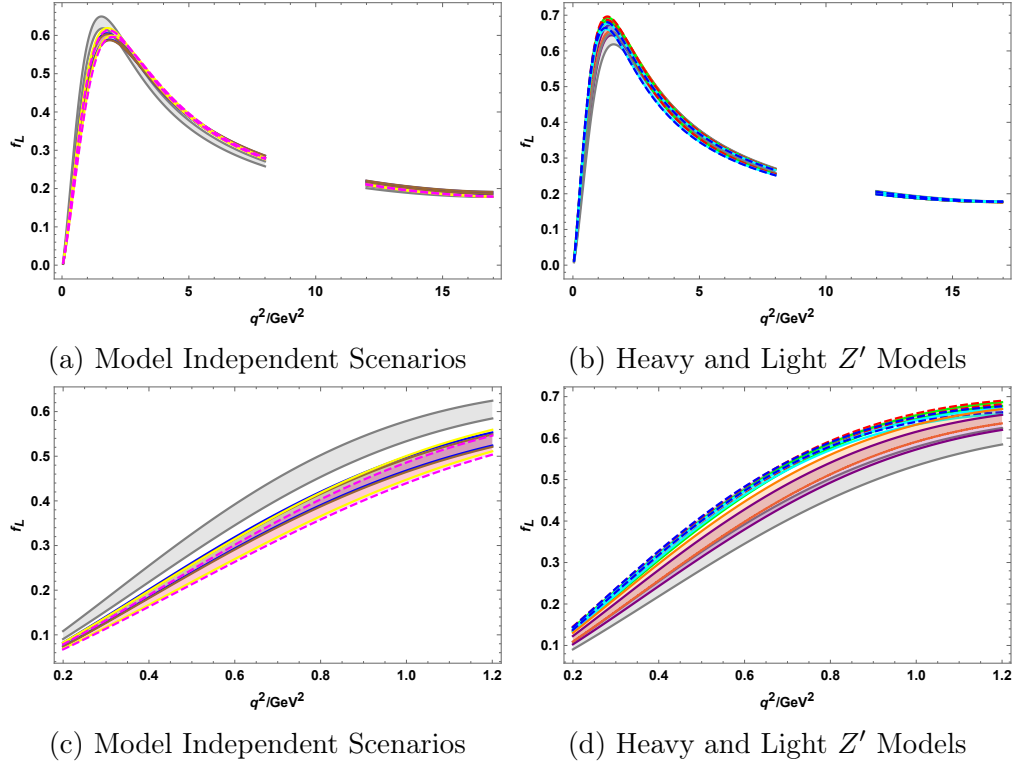


Figure 4.4: Longitudinal helicity fraction of  $D_s^*$  in MI Scenarios, LQ Model, Heavy  $Z'$  Model and Light  $Z'$  Model. The legends are same as in fig.4.2

Table 4.4: Predictions in SM and NP: Lepton flavor universality ratios  $R_{D_s^*}$  in different bin values for  $B_c \rightarrow D_s^* \mu^+ \mu^-$ .

| Scenarios      | low $q^2/\text{GeV}^2$ [0.045,1] | central $q^2/\text{GeV}^2$ [1,6] | high $q^2/\text{GeV}^2$ [ 14, max] |
|----------------|----------------------------------|----------------------------------|------------------------------------|
| SM             | $0.939 \pm 0.001$                | $0.985 \pm 0.0001$               | 0.996                              |
| MI, I(A)       | $0.941 \pm 0.001$                | $0.984 \pm 0.0001$               | 0.996                              |
| MI, LQ, II(A)  | $0.939 \pm 0.001$                | $0.986 \pm 0.0001$               | 0.996                              |
| MI, I(B)       | $0.941 \pm 0.001$                | $0.984 \pm 0.0001$               | 0.996                              |
| MI, LQ, II(A)  | $0.939 \pm 0.001$                | $0.986 \pm 0.0001$               | 0.996                              |
| TeV $Z'$ I(A)  | $0.939 \pm 0.001$                | $0.987 \pm 0.0001$               | 0.997                              |
| TeV $Z'$ II(A) | $0.939 \pm 0.001$                | $0.987 \pm 0.0001$               | 0.997                              |
| TeV $Z'$ I(B)  | $0.939 \pm 0.001$                | $0.985 \pm 0.0001$               | 0.997                              |
| TeV $Z'$ II(B) | $0.939 \pm 0.001$                | $0.985 \pm 0.0001$               | 0.997                              |
| GeV $Z'$ I(A)  | $0.938 \pm 0.002$                | $0.987 \pm 0.0001$               | 0.997                              |
| GeV $Z'$ II(A) | $0.938 \pm 0.002$                | $0.987 \pm 0.0001$               | 0.997                              |

Table 4.5: Predictions in SM and NP: Lepton flavor universality ratios  $R_{D_s^*}^L$  in different bin values for  $B_c \rightarrow D_s^* \mu^+ \mu^-$ .

| Scenarios      | low $q^2/\text{GeV}[0.045,1]$ | central $q^2/\text{GeV}[1,6]$ | high $q^2/\text{GeV}[14, \text{max}]$ |
|----------------|-------------------------------|-------------------------------|---------------------------------------|
| SM             | $0.752 \pm 0.005$             | $0.986 \pm 0.001$             | 0.997                                 |
| MI, I(A)       | $0.698 \pm 0.004$             | $0.982 \pm 0.0002$            | 0.996                                 |
| MI, LQ, II(A)  | $0.743 \pm 0.004$             | $0.986 \pm 0.0002$            | 0.997                                 |
| MI, I(B)       | $0.696 \pm 0.004$             | $0.982 \pm 0.0002$            | 0.996                                 |
| MI, LQ, II(A)  | $0.742 \pm 0.004$             | $0.985 \pm 0.0002$            | 0.997                                 |
| TeV $Z'$ I(A)  | $0.801 \pm 0.004$             | $0.990 \pm 0.0001$            | 0.997                                 |
| TeV $Z'$ II(A) | $0.803 \pm 0.005$             | $0.990 \pm 0.0001$            | 0.997                                 |
| TeV $Z'$ I(B)  | $0.762 \pm 0.004$             | $0.987 \pm 0.0001$            | 0.997                                 |
| TeV $Z'$ II(B) | $0.763 \pm 0.005$             | $0.987 \pm 0.0001$            | 0.997                                 |
| GeV $Z'$ I(A)  | $0.783 \pm 0.004$             | $0.989 \pm 0.0001$            | 0.997                                 |
| GeV $Z'$ II(A) | $0.794 \pm 0.004$             | $0.990 \pm 0.0001$            | 0.998                                 |

Table 4.6: Predictions in SM and NP: Lepton flavor universality ratios  $R_{D_s^*}^T$  in different bin values for  $B_c \rightarrow D_s^* \mu^+ \mu^-$ .

| Scenarios      | low $q^2/\text{GeV}[0.045,1]$ | central $q^2/\text{GeV}[1,6]$ | high $q^2/\text{GeV}[14, \text{max}]$ |
|----------------|-------------------------------|-------------------------------|---------------------------------------|
| SM             | $0.920 \pm 0.002$             | 0.983                         | 0.996                                 |
| MI, I(A)       | $0.920 \pm 0.001$             | 0.984                         | 0.996                                 |
| MI, LQ, II(A)  | $0.920 \pm 0.001$             | 0.984                         | 0.996                                 |
| MI, I(B)       | $0.920 \pm 0.001$             | 0.984                         | 0.996                                 |
| MI, LQ, II(A)  | $0.920 \pm 0.001$             | 0.984                         | 0.996                                 |
| TeV $Z'$ I(A)  | $0.922 \pm 0.002$             | 0.983                         | 0.997                                 |
| TeV $Z'$ II(A) | $0.922 \pm 0.002$             | 0.983                         | 0.997                                 |
| TeV $Z'$ I(B)  | $0.921 \pm 0.002$             | 0.982                         | 0.996                                 |
| TeV $Z'$ II(B) | $0.922 \pm 0.002$             | 0.982                         | 0.996                                 |
| GeV $Z'$ I(A)  | $0.938 \pm 0.002$             | 0.983                         | 0.997                                 |
| GeV $Z'$ II(A) | $0.938 \pm 0.002$             | 0.983                         | 0.997                                 |



Table 4.7: Predictions in SM and NP: Longitudinal helicity fraction  $F_{D_s^*}^L$  in different bin values for  $B_c \rightarrow D_s^* \mu^+ \mu^-$ .

| Scenarios      | low $q^2/\text{GeV}[0.045,1]$ | central $q^2/\text{GeV}[1,6]$ | high $q^2/\text{GeV}[14, \text{max}]$ |
|----------------|-------------------------------|-------------------------------|---------------------------------------|
| SM             | $0.177 \pm 0.002$             | $0.458 \pm 0.0008$            | 0.183                                 |
| MI, I(A)       | $0.133 \pm 0.001$             | $0.454 \pm 0.001$             | 0.192                                 |
| MI, LQ, II(A)  | $0.126 \pm 0.001$             | $0.460 \pm 0.001$             | 0.184                                 |
| MI, I(B)       | $0.131 \pm 0.001$             | $0.454 \pm 0.001$             | 0.193                                 |
| MI, LQ, II(A)  | $0.122 \pm 0.001$             | $0.460 \pm 0.001$             | 0.184                                 |
| TeV $Z'$ I(A)  | $0.229 \pm 0.016$             | $0.465 \pm 0.011$             | 0.181                                 |
| TeV $Z'$ II(A) | $0.227 \pm 0.016$             | $0.453 \pm 0.011$             | 0.182                                 |
| TeV $Z'$ I(B)  | $0.232 \pm 0.016$             | $0.465 \pm 0.011$             | 0.181                                 |
| TeV $Z'$ II(B) | $0.232 \pm 0.016$             | $0.452 \pm 0.011$             | 0.182                                 |
| GeV $Z'$ I(A)  | $0.202 \pm 0.015$             | $0.465 \pm 0.011$             | 0.181                                 |
| GeV $Z'$ II(A) | $0.217 \pm 0.015$             | $0.467 \pm 0.011$             | 0.181                                 |

Table 4.8: Predictions in SM and NP: Forward backward asymmetry  $A_{FB}$  in different bins for  $B_c \rightarrow D_s^* \mu^+ \mu^-$

| Scenarios      | low $q^2/\text{GeV}[0.045,1]$ | central $q^2/\text{GeV}[1,6]$ | high $q^2/\text{GeV}[14, \text{max}]$ |
|----------------|-------------------------------|-------------------------------|---------------------------------------|
| SM             | $-0.023 \pm 0.001$            | 0.001                         | $0.0421 \mp 0.001$                    |
| MI, I(A)       | $-0.024 \pm 0.0002$           | $-0.025 \mp 0.001$            | $0.035 \mp 0.001$                     |
| MI, LQ, II(A)  | $-0.020 \pm 0.0002$           | $-0.011 \mp 0.001$            | $0.041 \mp 0.001$                     |
| MI, I(B)       | $-0.024 \pm 0.0002$           | $-0.026 \mp 0.001$            | $0.034 \mp 0.001$                     |
| MI, LQ, II(B)  | $-0.020 \pm 0.0002$           | $-0.012 \mp 0.001$            | $0.041 \mp 0.001$                     |
| TeV $Z'$ I(A)  | $-0.021 \pm 0.0001$           | $0.017 \mp 0.001$             | $0.043 \mp 0.001$                     |
| TeV $Z'$ II(A) | $-0.025 \pm 0.0001$           | $0.010 \mp 0.001$             | $0.042 \mp 0.001$                     |
| TeV $Z'$ I(B)  | $-0.021 \pm 0.0002$           | $0.018 \mp 0.001$             | $0.043 \mp 0.001$                     |
| TeV $Z'$ II(B) | $-0.025 \pm 0.0001$           | $0.011 \mp 0.001$             | $0.042 \mp 0.001$                     |
| GeV $Z'$ I(A)  | $-0.021 \pm 0.0003$           | $0.012 \mp 0.001$             | $0.043 \mp 0.001$                     |
| GeV $Z'$ II(A) | $-0.021 \pm 0.0003$           | $0.016 \mp 0.001$             | $0.043 \mp 0.001$                     |

## Conclusion

Motivated by the anomalies present in  $B \rightarrow D^{(*)}\tau\nu$  and  $B \rightarrow K^{(*)}\mu^+\mu^-$  decays. like mentioned decays which are precisely discussed in literature, the decay  $B_c \rightarrow D_s^*\ell^+\ell^-$  also provide complimentary information regarding NP. We studied  $B_c \rightarrow D_s^*\ell^+\ell^-$  decay based on transition  $b \rightarrow s\ell^+\ell^-$  at quark level. In our study, we performed in SM and beyond. We added NP effects in said decay by the modification of wilson coefficients, used two different approaches to search NP effects including the model independent new physics scenarios (I) and (II), and in model dependent, we search NP effects by two different models leptoquark model and  $Z'$  models which involve tree level exchange of new bosonic particle. We analyzed several observables in said decay such as, branching ratios, longitudinal helicity fraction of  $D_s^*$  meson, forward backward asymmetry of lepton and lepton flavor universality (LFU) ratio which hint the influence of NP in said process.

We determined that for MI new physics scenarios and leptoquark model, the branching ratio for the decay is decreased at all  $q^2$  and for  $Z'$  models, the branching ratio for the said decay is increased at all  $q^2$  from SM prediction as shown in fig.4.2.

The zero value of leptons forward backward asymmetry  $A_{FB}(q^2)$  is shifted to higher values of  $q^2$  than in the standard model for model independent NP scenarios and leptoquark model, and for  $Z'$  models, it is shifted to lower values of  $q^2$  than in SM as shown in fig.4.3.

We analyze the longitudinal helicity fraction of the  $D_s^*$  meson for MI new physics scenarios and leptoquark model, the peak of the distribution is decreased at all  $q^2$  and it is shifted nearly higher value of  $q^2$  than in the SM, and for  $Z'$  Model, the peak of the distribution is increased from SM prediction as shown in fig.4.4.

The average  $q^2$  bin values of polarized LFU ratios are performed in low  $0.045 < q^2 < 1$  bin values have shown deviation from SM predictions which hint the influence of NP in said process.

Consequently, the deviation in all above mentioned observables from SM predictions is a good sign of the presence of NP in said decay. These predictions can be tested at the LHC and can add information regarding NP in  $b \rightarrow s\ell^+\ell^-$  decay.

# Bibliography

- [1] A. K. Alok, B. Bhattacharya, A. Datta, D. Kumar, J. Kumar, and D. London, “New Physics in  $b \rightarrow s\mu^+\mu^-$  after the Measurement of  $R_{K^*}$ ,” *Phys. Rev. D*, vol. 96, no. 9, p. 095009, 2017.
- [2] I. Ahmed, M. Paracha, M. Junaid, A. Ahmed, A. Rehman, and M. Aslam, “Analysis of  $B_c \rightarrow D_s^*\ell^+\ell^-$  in the Standard Model Beyond Third Generation,” 7 2011.
- [3] W.-L. Ju, G.-L. Wang, H.-F. Fu, T.-H. Wang, and Y. Jiang, “The study of rare decays,” *Journal of High Energy Physics*, vol. 2014, no. 4, p. 1, 2014.
- [4] M. K. Gaillard, P. D. Grannis, and F. J. Sciulli, “The standard model of particle physics,” *Reviews of Modern Physics*, vol. 71, no. 2, p. S96, 1999.
- [5] S. Cho, P. Ko, J. Lee, Y. Omura, and C. Yu, “Top fcnc induced by a  $z'$  boson,” *Physical Review D*, vol. 101, no. 5, p. 055015, 2020.
- [6] S. L. Glashow, J. Iliopoulos, and L. Maiani, “Weak interactions with lepton-hadron symmetry,” *Physical review D*, vol. 2, no. 7, p. 1285, 1970.
- [7] M. Artuso, E. Barberio, and S. Stone, “B meson decays, pmc phys,” 2009.
- [8] J. Charles, A. Höcker, H. Lacker, S. Laplace, F. Le Diberder, J. Malclès, J. Ocariz, M. Pivk, and L. Roos, “Cp violation and the ckm matrix: Assessing the impact of the asymmetric b factories,” *The European Physical Journal C-Particles and Fields*, vol. 41, no. 1, pp. 1–131, 2005.
- [9] C. Quigg, *Gauge theories of the strong, weak, and electromagnetic interactions*. Princeton University Press, 2013.
- [10] C. Delaere, *Study of WW decay of a Higgs boson with the ALEPH and CMS detectors*. PhD thesis, Leuven U., 2005.
- [11] S. Weinberg, “A Model of Leptons,” *Phys. Rev. Lett.*, vol. 19, pp. 1264–1266, 1967.

- [12] C. Burgess and G. Moore, *The standard model: A primer*. Cambridge University Press, 2006.
- [13] J. Bernstein, “Spontaneous symmetry breaking, gauge theories, the higgs mechanism and all that,” *Reviews of modern physics*, vol. 46, no. 1, p. 7, 1974.
- [14] K. Nakamura, P. D. Group, *et al.*, “Review of particle physics,” *Journal of Physics G: Nuclear and Particle Physics*, vol. 37, no. 7A, p. 075021, 2010.
- [15] M. Neubert, “Effective field theory and heavy quark physics,” in *Physics In  $D \geq 4$  Tasi 2004: TASI 2004*, pp. 149–194, World Scientific, 2006.
- [16] I. Z. Rothstein, “Tasi lectures on effective field theories,” *arXiv preprint hep-ph/0308266*, 2003.
- [17] A. Faessler, T. Gutsche, M. Ivanov, J. Korner, and V. E. Lyubovitskij, “The Exclusive rare decays  $B \rightarrow K(K^*) \bar{\ell}\ell$  and  $B_c \rightarrow D(D^*) \bar{\ell}\ell$  in a relativistic quark model,” *Eur. Phys. J. direct*, vol. 4, no. 1, p. 18, 2002.
- [18] F. Lattice, M. Collaborations, D. Du, A. El-Khadra, S. Gottlieb, A. Kronfeld, J. Laiho, E. Lunghi, R. Van de Water, and R. Zhou, “Phenomenology of semileptonic b-meson decays with form factors from lattice qcd,” *Physical Review D*, vol. 93, no. 3, p. 034005, 2016.
- [19] S. Jäger, M. Kirk, A. Lenz, and K. Leslie, “Charming new b-physics,” *Journal of High Energy Physics*, vol. 2020, no. 3, pp. 1–40, 2020.
- [20] A. K. Alok, B. Bhattacharya, D. Kumar, J. Kumar, D. London, and S. U. Sankar, “New physics in  $b \rightarrow s\mu^+\mu^-$ : Distinguishing models through CP-violating effects,” *Phys. Rev. D*, vol. 96, no. 1, p. 015034, 2017.
- [21] S. Sahoo and R. Mohanta, “Scalar leptoquarks and the rare  $B$  meson decays,” *Phys. Rev. D*, vol. 91, no. 9, p. 094019, 2015.
- [22] L. Calibbi, A. Crivellin, and T. Ota, “Effective Field Theory Approach to  $b \rightarrow s\ell\ell^{(\prime)}$ ,  $B \rightarrow K^{(*)}\nu\bar{\nu}$  and  $B \rightarrow D^{(*)}\tau\nu$  with Third Generation Couplings,” *Phys. Rev. Lett.*, vol. 115, p. 181801, 2015.
- [23] R. Alonso, B. Grinstein, and J. Martin Camalich, “Lepton universality violation and lepton flavor conservation in  $B$ -meson decays,” *JHEP*, vol. 10, p. 184, 2015.
- [24] G. Hiller and M. Schmaltz, “ $r_k$  and future  $b \rightarrow s\ell\ell$  physics beyond the standard model opportunities,” *Physical Review D*, vol. 90, no. 5, p. 054014, 2014.
- [25] S. Sahoo and R. Mohanta, “Scalar leptoquarks and the rare b meson decays,” in *XXI DAE-BRNS High Energy Physics Symposium*, pp. 221–226, Springer, 2016.
- [26] S. Fajfer and N. Košnik, “Vector leptoquark resolution of  $r_k$  and  $r_d^{(*)}$  puzzles,” *Physics Letters B*, vol. 755, pp. 270–274, 2016.

- [27] I. Ahmed and A. Rehman, “LHCb anomaly in  $B \rightarrow K^* \mu^+ \mu^-$  optimised observables and potential of  $Z'$  Model,” *Chin. Phys. C*, vol. 42, no. 6, p. 063103, 2018.
- [28] V. Barger, C.-W. Chiang, P. Langacker, and H.-S. Lee, “ $Z'$  mediated flavor changing neutral currents in  $B$  meson decays,” *Phys. Lett. B*, vol. 580, pp. 186–196, 2004.
- [29] A. J. Buras, F. De Fazio, and J. Girrbach, “The Anatomy of  $Z'$  and  $Z$  with Flavour Changing Neutral Currents in the Flavour Precision Era,” *JHEP*, vol. 02, p. 116, 2013.
- [30] V. Barger, L. L. Everett, J. Jiang, P. Langacker, T. Liu, and C. E. Wagner, “ $b \rightarrow s$  transitions in family-dependent  $U(1)'$  models,” *JHEP*, vol. 12, p. 048, 2009.
- [31] A. Ali, P. Ball, L. Handoko, and G. Hiller, “Comparative study of the decays  $b \rightarrow (k, k^*) l^+ l^-$  in the standard model and supersymmetric theories,” *Physical Review D*, vol. 61, no. 7, p. 074024, 2000.
- [32] R. Aaij *et al.*, “Test of lepton universality using  $B^+ \rightarrow K^+ \ell^+ \ell^-$  decays,” *Phys. Rev. Lett.*, vol. 113, p. 151601, 2014.
- [33] R. Aaij *et al.*, “Test of lepton universality with  $B^0 \rightarrow K^{*0} \ell^+ \ell^-$  decays,” *JHEP*, vol. 08, p. 055, 2017.
- [34] B. Dey, “Lepton Flavor Universality tests in  $b \rightarrow s \ell^+ \ell^-$  decays at LHCb,” *PoS*, vol. ICHEP2018, p. 069, 2019.